



Cite this: *Org. Biomol. Chem.*, 2021,  
**19**, 1168

Received 18th November 2020,  
Accepted 5th January 2021

DOI: 10.1039/d0ob02299c

rsc.li/obc

## Silicon phthalocyanines: synthesis and resurgent applications

Koushambi Mitra <sup>a,b</sup> and Matthew C. T. Hartman <sup>a,b</sup>

The intense far-red absorption and emission features have made silicon phthalocyanines (SiPcs) distinct from the structurally related porphyrin analogues. Unlike most other phthalocyanines, SiPcs possess two additional axial bonds which reduce aggregation in solution and can be synthetically tailored, thereby creating further scope for modulation of optical, chemical and electronic properties. Multiple synthetic strategies have been employed for facile construction of symmetrical or unsymmetrical SiPc variants bearing desired substituents at the axial and the aromatic ring positions. The overarching motive of this concise review article is to highlight and summarize the key synthetic routes and the fast-emerging applications of SiPcs in photouncaging techniques, photothermal and photoimmunotherapy, photovoltaics, optoelectronics and photocatalysis.

### 1. Introduction

The mid-twentieth century witnessed a wave of enthusiasm among researchers in developing new classes of macroheterocyclic compounds by inserting different elements in the core of phthalocyanines (Pcs).<sup>1–4</sup> Like their closely related por-

<sup>a</sup>Department of Chemistry, Virginia Commonwealth University, 1001 W Main St, Richmond, 23284 VA, USA

<sup>b</sup>Massey Cancer Center, Virginia Commonwealth University, 401 College St, Richmond, 23219 Virginia, USA. E-mail: mchartman@vcu.edu, kmitrachem@gmail.com; Tel: +1-804-628-4095



**Koushambi Mitra**

Koushambi Mitra graduated from Presidency College, University of Calcutta, India in 2009 with a B.Sc. degree in chemistry. She obtained her integrated Ph.D. degree from Indian Institute of Science in 2016. Her doctoral thesis focused on development of visible light-activated platinum(II) complexes as dual-action photo-chemotherapeutic anticancer agents. She undertook postdoctoral studies in Virginia Commonwealth University where she explored synthesis of near-infrared photocages and their applications as cancer drug delivery systems. She then transitioned to The University of Texas at Dallas, where she developed activity-based fluorescent sensors for live cell imaging of the phase II metabolic enzymes, sulfotransferases. Currently, she is a postdoctoral researcher at The University of Chicago and her research involves development of quantitative imaging platforms for studying cations and anions in organelles of living systems.



**Matthew C. T. Hartman**

Matthew C. T. Hartman received his Ph.D. degree from the University of Michigan in 2002, studying under Professor James Coward. He was then a HHMI postdoctoral fellow with Professor Jack Szostak at Harvard University (2002–2006). Since 2007 he has been at Virginia Commonwealth University where he currently is an Associate Professor in the Department of Chemistry and the Massey Cancer Center. His research interests focus on the discovery of natural-product like peptide inhibitors of protein–protein interactions and the delivery and activation of chemotherapeutic agents with light.



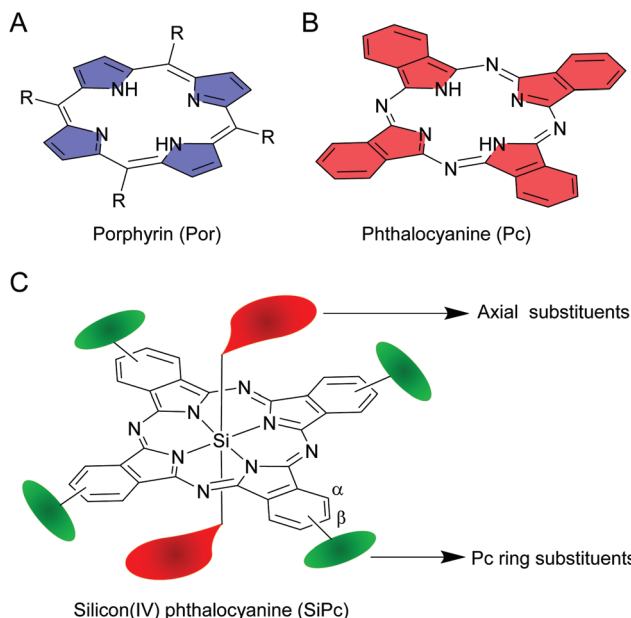


**Fig. 1** Chemical structures of (A) porphyrin (Por), (B) phthalocyanine (Pc) and (C) silicon(IV) phthalocyanine (SiPc). R denotes various alkyl or aryl groups. The axial substituents are highlighted as red teardrops. The phthalocyanine ring ( $\alpha$ ) and ( $\beta$ ) substituents are highlighted as green ovals.

porphyrin (Por) analogues, Pcs are also 18  $\pi$ -electronic systems. However, a Pc construct has imine bridges and isoindole rings as opposed to the methine bridges and pyrrole rings of a Por structure (Fig. 1A and B).<sup>5</sup> Due to these structural variations, Pcs exhibit intense absorption at  $\sim$ 700 nm (Q-band), and thus qualify as one of the elite classes of far-red light absorbing organic compounds. Further modification by replacing benzenes with naphthalenes as the peripheral rings results in the formation of naphthalocyanines (Ncs).<sup>6,7</sup> Due to increase in  $\pi$ -delocalization, Q-bands of Ncs are red shifted by  $\sim$ 100 nm compared to Pcs, and thus, these dyes classify as near-infrared (NIR) absorbing dyes. Despite their interesting optical properties in the visible, red and NIR region, the applications of these hydrophobic planar molecules were not fully realized because of poor solubility and tendency to form aggregates. Aggregate formation quenches excited state lifetimes and diminishes photophysical properties.<sup>8,9</sup> Structural variations such as incorporation of appropriate aromatic substitutions or an element in the core structure were sought after to reduce the degree of planarity and hydrophobicity.<sup>10–12</sup> These attempts have led to the development of facile synthetic routes for a new generation of Pcs with improved solubility, reduced aggregation, interesting photophysical and photochemical properties.

Amidst all core-substituted Pcs, silicon phthalocyanines (SiPcs) immediately caught attention because of the unusual hexacoordinated silicon(IV) and marked chemical stability of the Si–N bonds.<sup>13</sup> Moreover, the presence of two unique axial positions which can be readily functionalized with ligands of choice rendered it unparalleled in the plethora of Pcs (Fig. 1C).

These axial ligands serve as pivotal handles for fine-tuning of the properties of SiPcs as desired. Furthermore, bulky or polar substitutions in the axial positions perturb planarity and are more effective than the  $\alpha$  or  $\beta$  phthalocyanine ring substitutions in reducing aggregation and improving solubility.<sup>14,15</sup> Extensive synthetic methodologies have been developed for preparation of symmetrical and unsymmetrical SiPcs, often containing both tetravalent (axial) and hexavalent (core) silicon in the same structure.<sup>16,17</sup> Remarkably, axial Si–O and Si–C bonds exhibit NIR light induced dissociation rendering novel applications of SiPcs in medicinal biology, beyond the context of photodynamic therapy.<sup>18–22</sup> These unique properties coupled with the inexpensive cost of synthesis and low toxicity have resulted in fascinating applications of SiPcs in major fields of research including cancer phototherapy, NIR imaging, organic photovoltaics, organic electronics and photocatalysis.

In this condensed review article, we present an overview of the broad synthetic methodologies adapted to improve the design of symmetrical and non-symmetrical SiPcs, since their first successful isolation in around 1960. Here, we also account for the interesting properties and the related applications of SiPcs over the past decade, emphasizing mostly on the emerging and novel applications. In the concluding section, we have included a brief perspective to provide guidance for rationally designing an envelope of new SiPc derivatives, to discern areas of impending developments, and to anticipate the future directions of this interesting field.

## 2. Syntheses of silicon phthalocyanines

Facile, short and high yielding synthetic strategies comprising of non-hazardous and easily accessible starting materials are an essential prerequisite to realize the complete potential of any material. Various synthetic approaches have been developed to increase the structural flexibility of SiPcs. These approaches offer easy modulation of the physico-chemical properties as desired and help to rapidly generate a vast library of SiPc derivatives with diverse functionalities and applications. For example, successful applications of SiPcs in biological fields can be achieved by incorporation of water soluble or biocompatible groups.<sup>11,23</sup> On the other hand, insertion of electron donating and electron withdrawing moieties can alter the opto-electronic properties of SiPc molecules.<sup>5,12</sup> Likewise, availability of electrophilic or nucleophilic reactive handles in the SiPc structure will allow to append desired functionalities for versatile applications.

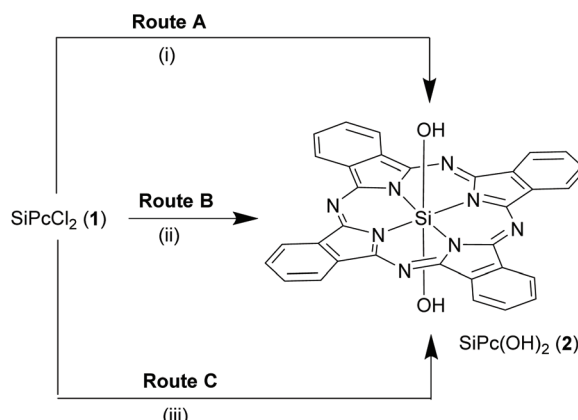
Such fine-tuning of SiPc structures is mainly obtained by reactions at two major sites: (i) the axial and (ii) the phthalocyanine ring ( $\alpha$ ) and ( $\beta$ ) positions (Fig. 1C). While the axial handles are exploited for imparting variants without considerably affecting the absorption and emissive properties of SiPc, the  $\alpha/\beta$  substitutions result in a prominent change of spectral features. Below, we have elaborated on the discovery of SiPc

and the various synthetic methods developed henceforth resulting in the formation of several symmetrical and unsymmetrical SiPcs.

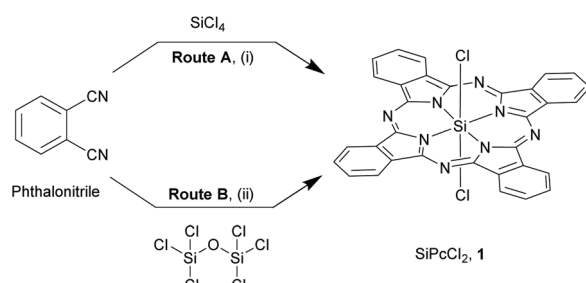
## 2.1 Synthesis of SiPc precursors

The synthesis of most SiPcs is based on two main precursors, the dichloro SiPc ( $\text{SiPcCl}_2$ ), **1** (Schemes 1 and 2) and the bis-hydroxy adduct ( $\text{SiPc}(\text{OH})_2$ , **2**, (Scheme 3). In this section, we have described the synthetic strategies for these important building blocks.

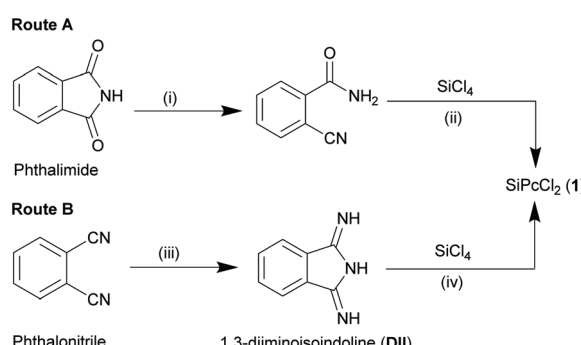
**2.1.1 Synthesis of dichloro SiPc ( $\text{SiPcCl}_2$ ).** Linstead and co-workers attempted but failed to synthesize SiPc using a direct reaction of Pcs with silicon tetrachloride ( $\text{SiCl}_4$ ).<sup>1</sup> Later, in a seminal report, Joyner and Kenney envisioned a different synthetic route involving 1,2-dicyanobenzene or phthalonitrile (a precursor extensively used for synthesis of Pcs) instead of a metal free Pcs as the starting material.<sup>24</sup> They exposed phthalonitrile to repeated treatments with  $\text{SiCl}_4$  for 2 h using dry quinoline as a solvent and a reaction temperature of  $>200\text{ }^\circ\text{C}$  (Route A, Scheme 1). Further purification using vacuum sublimation techniques resulted in formation of blue-green crystals which were presumed to be the desired dichloro SiPc analogue ( $\text{SiPcCl}_2$ ), **1** (Scheme 1). Use of hexachlorodisiloxane instead of



**Scheme 3** Synthetic routes for hydrolysis of the axial chloro bonds to form bis-hydroxyl SiPc derivative, **2**. Reagents and conditions: (i) 1:1 (v/v) pyridine and conc. aq.  $\text{NH}_3$ , 10 h, reflux; (ii) large excess of conc.  $\text{H}_2\text{SO}_4$ , r.t.; (iii)  $\text{NaOCH}_3$ , 95% ethanol, reflux, 1 h.



**Scheme 1** Early synthetic routes for silicon phthalocyanines, **1**. Reagents and conditions: (i)  $\text{SiCl}_4$ , dry quinoline,  $>200\text{ }^\circ\text{C}$ , 2 h; (ii) hexachlorodisiloxane, dry quinoline, reflux, 4 h.



**Scheme 2** Synthetic routes for obtaining  $\text{SiPcCl}_2$  (1) starting from precursors phthalimide and phthalonitrile. Reagents and conditions: (i) conc. ammonium hydroxide, 24 h, r.t. (ii)  $\text{SiCl}_4$ , dry quinoline, dry 1,2-dichlorobenzene,  $205\text{ }^\circ\text{C}$ , 5 min; (iii) (a)  $\text{NH}_3$  gas,  $\text{NaOCH}_3$ , methanol, 40 min, r.t.; (b) reflux, 3.2 h; (iv)  $\text{SiCl}_4$ , dry quinoline, reflux ( $219\text{ }^\circ\text{C}$ ), 30 min.

$\text{SiCl}_4$  as the source of silicon also resulted in improved yields of **1** under similar conditions, which was purified by Soxhlet extraction process (Route B, Scheme 1).<sup>13</sup> However, similar attempts to synthesize **1** by reacting organo chlorosilanes such as methyltrichlorosilane and phenyltrichlorosilane with phthalonitrile were unsuccessful.<sup>13</sup> Interestingly, the Si–N bonds exhibited unprecedented stability under extreme acidic or basic conditions.

Though Kenney and co-workers successfully isolated this extraordinary class of compounds, the initial synthetic routes were experimentally inconvenient due to poor yields and laborious purification methods. This entailed exploration of refined strategies with alternate starting materials and/or inclusion of additional reaction steps. Reaction of 2-cyanobenzamide (obtained from hydrolysis of phthalimide with concentrated ammonium hydroxide) with  $\text{SiCl}_4$  in quinoline at elevated temperatures ( $\sim 205\text{ }^\circ\text{C}$ ) resulted in the formation of a blue solid (Route A, Scheme 2).<sup>25</sup> The crude precipitate was washed with quinoline, benzene, pyridine, acetic acid, ethanol and ether to obtain the pure **1** (yield  $\sim 35\%$ ). Another two-step synthetic route comprised of ammonolysis of phthalonitrile in methanol and sodium methoxide to form 1,3-diiminoisoindoline (**DII**) in the initial step, followed by reflux of **DII** with  $\text{SiCl}_4$  in quinoline to afford compound **1** (yield  $\sim 71\%$ ) (Route B, Scheme 2).<sup>25</sup>

Brusso and co-workers recently proposed an alternate route to synthesize **DII** from phthalonitrile by using air-stable lithium bis(trimethylsilyl)amide etherate,  $\text{LiN}(\text{TMDS})_2 \cdot \text{Et}_2\text{O}$  in dry toluene at room temperature for 5 h, followed by exposure to gaseous hydrochloric acid at ice bath temperature.<sup>26</sup> The dichloride salt,  $\text{H}_2\text{DIICl}_2$ , thus formed when refluxed with  $\text{SiCl}_4$  in quinoline afforded **1** (yield  $\sim 51\%$ ). Among all these synthetic pathways, route B of Scheme 2 remains the most convenient and preferred choice for the construction of SiPcs.

The axial chloro groups of SiPc **1** can be replaced with other halogens. The chlorides are replaced by fluoride atoms on treat-



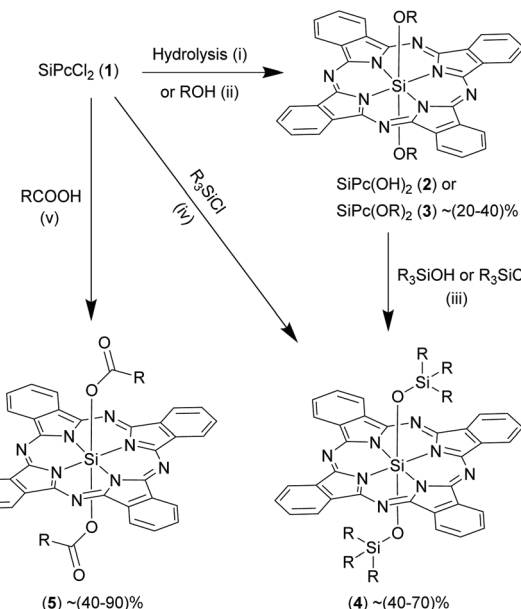
ment with 49% hydrofluoric acid (HF) on a steam bath, and resulted in the formation of  $\text{SiPcF}_2$ .<sup>27,28</sup> Recently, Bender and co-workers synthesized  $\text{SiPcF}_2$  by refluxing **1** with either cesium fluoride (CsF) in dimethylformamide or with tetrabutylammonium fluoride in dimethyl sulfoxide.<sup>29</sup> These alternate strategies involved relatively safer fluorinating agents compared to HF and resulted in high reaction yields of 100% and 73% respectively. In a similar approach, boron tribromide was used as a brominating reagent for the synthesis of  $\text{SiPcBr}_2$ .<sup>27</sup>

**2.1.2 Synthesis of  $\text{SiPc(OH)}_2$ , 2.** It was observed that the Si-Cl bonds of **1** can undergo hydrolysis. Compound **1** when refluxed with pyridine and concentrated aqueous ammonia (1:1 v/v mixture) for 10 h<sup>13,24</sup> or treated with large excess of concentrated sulfuric acid at room temperature followed by dilution with water, hydrolysed to form  $\text{SiPc(OH)}_2$ , **2** in ~80% yield (Routes A and B, Scheme 3).<sup>13</sup> Alternatively, sodium methoxide in 5% aqueous-ethanol hydrolysed **1** under reflux conditions to yield **2** (~83%) and provided a comparatively safer method (Route C, Scheme 3).<sup>25</sup> A recent report used 50% aqueous cesium hydroxide in DMF to obtain **2** from **1**.<sup>30</sup> Interestingly, unlike ordinary silanols, the axial hydroxyl groups of  $\text{SiPc}$  **2** are less acidic in nature and require harsh reaction conditions for deprotonation.<sup>13</sup>

## 2.2 Synthesis of SiPcs with axial substitutions

**2.2.1 Synthesis of symmetrical SiPcs with axial Si-OR bonds.** Compounds **1** and **2** can be further fabricated by substituting the unique axial chloro and hydroxyl groups by alcohols, phenols, silanols, chlorosilanes and carboxylic acids to generate the compounds **3–5** (Scheme 4). The axial Si-Cl bonds in **1** undergo smooth reactions with alcohols and phenols to generate the corresponding symmetrically substituted bis-alkoxy derivatives, **3**. Such reactions are reported with phenols (such as 2-naphthol, 1-naphthol, phenol, 4-hydroxybenzaldehyde, 4-aminophenol, 4-nitrophenol, 4-hydroxypyridine and 3-hydroxypyridine) as well as other hydroxylic compounds (such as solketal, polyethylene glycols, 1,3-bis(dimethylamino)-2-propanol and mono-6-hydroxy permethylated  $\beta$ -cyclodextrin). In a typical reaction, **1** was refluxed with 3–7 times excess ROH ( $R =$  alkyl, aryl groups) at ~120 °C in dry solvents like toluene or dichlorobenzene for about 24–96 h.<sup>14,20,27,31–38</sup> Reactions proceeded under argon atmosphere in presence of ~10 times excess of a base such as sodium hydride or dry pyridine (Scheme 4). Generally, small volumes of solvent were used to accelerate the precipitation of the blue-coloured bis-alkoxy SiPc products. The yields of these reactions varied from 20–40% depending on the nature of the  $R$  groups.

In order to form a siloxane bond in the axial position, precursor **2** is refluxed with an excess of silanols or monochlorosilanes to obtain **4** (yields ~40–70%).<sup>13,16,17,39–42</sup> Reactions were usually carried out for short durations ranging from 3–6 h in non-polar solvents (e.g. dichlorobenzene and toluene) in presence of a mild base (e.g. pyridine) (Scheme 4).<sup>6,16,39</sup> Interestingly, the axial Si-O-R linkages in certain bis-alkoxy SiPc derivatives, **3**, can react with silanols under reflux conditions in dry pyridine to generate siloxane (Si-O-Si) bonds thereby



**Scheme 4** Reactions of  $\text{SiPcCl}_2$ , **1** where axial chlorides are replaced by alcohols, phenols, silanes and carboxylic acids. Reagents and conditions: (i)  $\text{NaOCH}_3$ , 95%  $\text{CH}_3\text{CH}_2\text{OH}$ , reflux, 1 h; (ii) ROH, toluene, pyridine or sodium hydride, reflux, 120 °C, 24–96 h; (iii)  $\text{R}_3\text{SiOH}$  or  $\text{R}_3\text{SiCl}$ , toluene, pyridine, reflux, 120 °C, 3–6 h; (iv)  $\text{R}_3\text{SiCl}$ , NaOH, Aliquat HTA-1, chlorobenzene, reflux, 132 °C; (v) RCOOH, methoxyethyl ether, reflux, 160 °C, 0.5–6 h. R represent aryl or alkyl groups.

forming SiPc derivatives, **4**.<sup>13,43</sup> Alternatively, **4** were obtained by directly refluxing **1** with trialkylchlorosilanes in sodium hydroxide and chlorobenzene in presence of Aliquat HTA-1, a high temperature phase transfer catalyst (Scheme 4).<sup>44</sup>

Oligomeric and polymeric SiPc derivatives having axial Si-O and Si-O-Si linkages have been reported as well. Such  $\mu$ -oxo bridged SiPc polymers were formed when compound **1** was allowed to react with **2** and the resulting hydroxy-capped oligomers were reacted with a chlorosilane.<sup>6</sup> The desired polymer was isolated by column chromatography. Another way to obtain oligomers is from reaction of **1** or **2** with dendritic hydroxylic compounds (e.g. polyethylene glycols and triethanolamines) or silanols containing multiple hydroxyl moieties in the axial position. The properties of these polymers were investigated in both solid and solvent phases and some of these derivatives were even processed into thin polymeric films.<sup>45–50</sup>

Attempts to react **1** with alternate ligand functionalities such as carboxylic acids were successful and expanded the domain of axial functionalization of SiPcs (Scheme 4).<sup>27</sup> Esterification reactions of **1** occurred under reflux conditions in polar solvents such as 2-methoxyethyl ether (~160 °C), diglyme (~160 °C) or 1,4-dioxane (~100 °C), DMF (~160 °C) to produce various SiPc esters, **5**. Unlike etherification, esterification reactions proceeded easily in the absence of a base. The reaction completion times ranged from as short as of 30 min to as long as 48 h.<sup>20,51–56</sup> The SiPc bis-esters, **5** were obtained as blue solids in moderate (~30%) to high (~90%) yields.



**2.2.2 Synthesis of unsymmetrical SiPcs with axial Si-OR bonds.** The strategies described in Scheme 4 have led to a wide array of axially functionalized symmetrical SiPcs, 3–5; however, in comparison to their symmetrical analogues, only a few SiPc derivatives with unsymmetrical axial Si–O bonds have been reported to date.

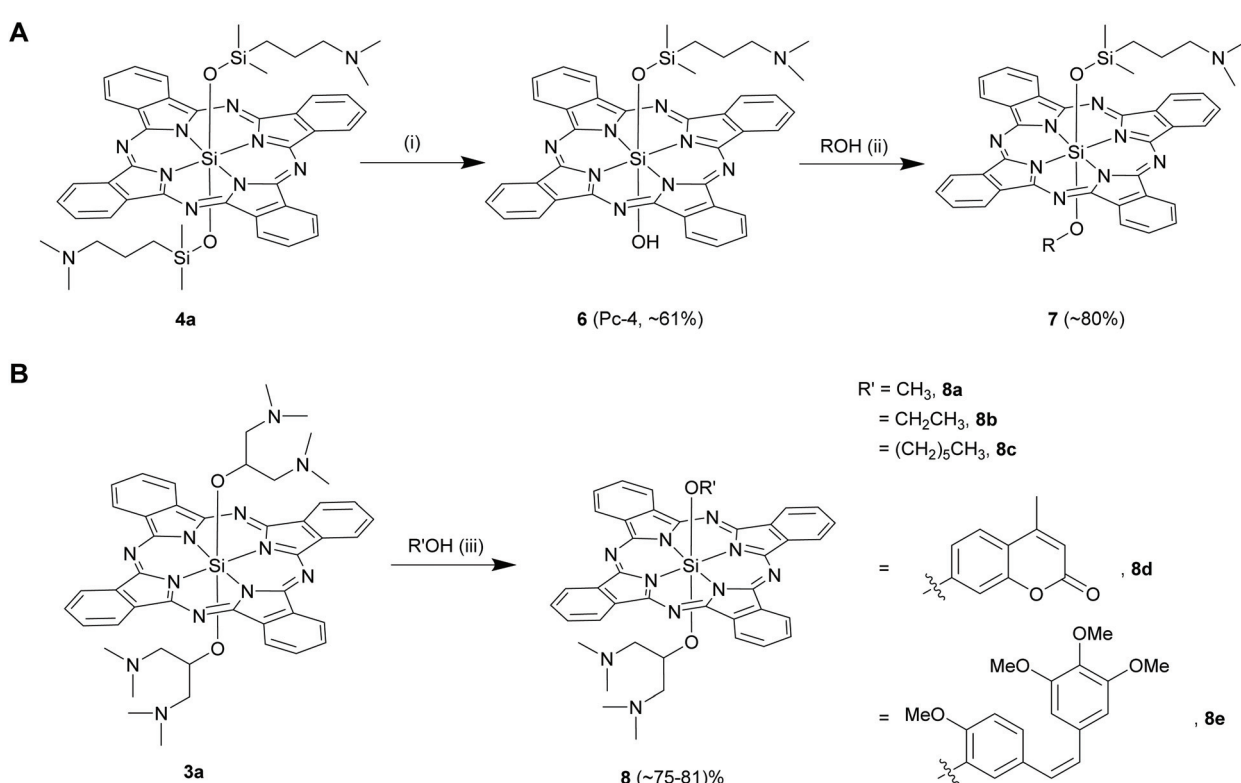
Kenney and co-workers noticed that only one of the two axial Si–O–Si linkages hydrolysed when **4a** ( $R = [(CH_3)_2Si(CH_2CH_2CH_2N(CH_3)_2)]$  in **4**) was stirred with trichloroacetic acid in dichloromethane at room temperature for 5 h (Scheme 5A).<sup>22,57</sup> This hydrolysed product, **6** was then reacted with methanol in dry pyridine to form unsymmetrical SiPc, **7** in high yields of ~80% (Scheme 5A). Another synthetic route to obtain **6** is strategized on exploiting the photolabile nature of Si–C bonds which will be discussed in the proceeding sections of organo SiPcs.<sup>58</sup>

In an endeavour to synthesize and explore amphiphilic SiPc derivatives as PDT agents, Ng and co-workers serendipitously discovered a facile route to prepare unsymmetrical SiPc derivatives having axial Si–O linkages (Scheme 5B).<sup>59</sup> In an attempt to purify a bis-alkoxy symmetrical SiPc, **3a** ( $R = 1,3\text{-bis}(\text{dimethylamino})\text{-2-propanol}$  in **3**) by crystallization from methanol–chloroform solvent at room temperature, they observed the formation of an unsymmetrical SiPc, **8a** in high reaction yields (~73%). Similar displacements reactions of **3a** occurred with

slight excess of ethanol and *n*-hexanol, but only under reflux conditions (~70 °C) in chloroform for 48 h to form **8b** and **8c** (yields ~29–37%). In contrast, no mono-substituted unsymmetrical SiPc could be isolated when **3a** was refluxed with dodecanol for 48 h. All these observations led to the conclusion that the length of the alkyl group of the alcohols played a crucial role in determining the ratio of the mono and di-substituted SiPc products, however their different reactivities were unaccounted. Recently, Schnermann and co-workers utilized this method and displaced one of the bulky axial ligands from **3a** with biologically relevant phenols such as coumarins and combretastatin to obtain SiPcs, **8d** and **8e** (Scheme 5B).<sup>19</sup> The use of phenols and prior neutralization of chloroform over anhydrous potassium carbonate possibly led to improved reaction yields of ~80%.

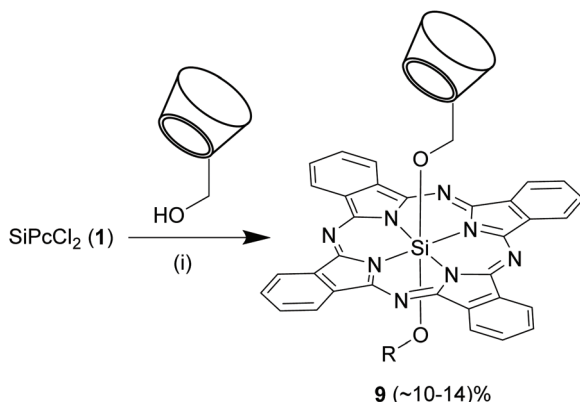
A recent report also utilized a similar displacement methodology to synthesize SiPc with unsymmetrical axial Si–OR bonds.<sup>60</sup> Oligomeric ethylene glycols of various lengths were incorporated in one of the axial positions by refluxing a symmetrical amino-containing bis-phenoxy SiPcs with large excess (40×) of desired glycols in toluene in presence of sodium hydride. Moderate yields of 23–31% were achieved using this strategy.

In another report, Ng and co-workers used a slightly different strategy to synthesize SiPcs with unsymmetrical axial



**Scheme 5** Synthesis of axially unsymmetrical Si–O bond containing SiPc derivatives starting from a symmetrical (A) bis-siloxy or (B) bis-ether SiPc compounds. Reagents and conditions: (i) (a) trichloroacetic acid, dichloromethane, r.t., 4 h (b) pyridine, water; (ii)  $CH_3OH$ , pyridine, reflux, 30 min; (iii)  $R'OH$ , chloroform, r.t. or 70–95 °C, 18–48 h. R and  $R'$  denotes aryl and alkyl groups as shown in the figure. Yield of 61% for Pc-4 is calculated based on initial starting material 2,  $SiPc(OH)_2$ .





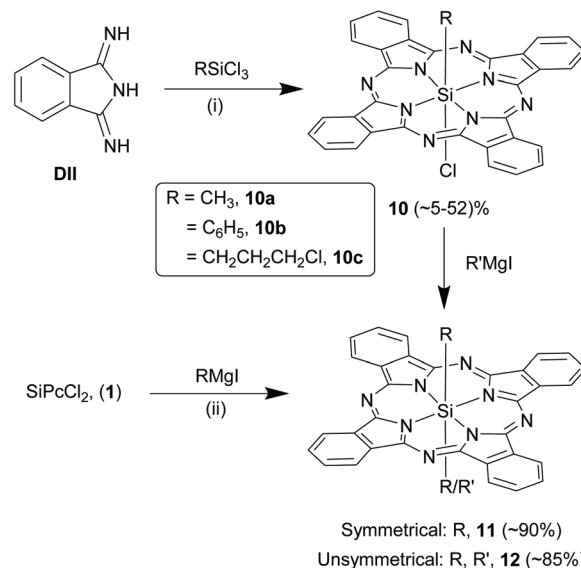
**Scheme 6** Synthesis of axially unsymmetrical Si–O bond containing SiPcs. Reagents and conditions: (i) (a) ROH, sodium hydride, toluene, r.t., 30 min, (b) 1, reflux, 1 h, (c) mono-6-hydroxy permethylated  $\beta$ -cyclodextrin (shown as cylindrical structure), sodium hydride, toluene, reflux, 48 h. R represents various alkyl moieties.

substituents, 9 (Scheme 6).<sup>61</sup> Compound 1 was initially refluxed with various alkyl alcohols bearing sugar or diamino moieties in dry toluene and sodium hydride. After an hour of reaction, mono-6-hydroxy permethylated  $\beta$ -cyclodextrin and sodium hydride were added to the mixture and the reaction was continued for another 48 h. In these reactions, 1 was always taken in 1.5-folds molar excess of that of the alcohols to prevent exclusive formation of axially symmetrical SiPcs. However, the reaction yields of 9 were comparatively low (10–14%).

SiPcs with unsymmetrical axial Si–O bonds have also been synthesized by selectively functionalizing one of the axial groups of a symmetrical SiPc. In a recent example, only one of the axial carboxylic acid groups in a symmetrical SiPc was subjected to a typical amide coupling reaction to form a series of unsymmetrical SiPc-peptide conjugates.<sup>62</sup>

### 2.2.3 Synthesis of SiPcs with axial Si–C bonds

*Symmetrical and unsymmetrical SiPcs with axial Si–C bonds.* The formation and isolation of SiPcs with direct Si–C axial bonds have been comparatively difficult because of two prime reasons: (i) cationic nature of hexa-coordinated silicon which instead prefers bonding with electronegative elements such as oxygen and chloride and (ii) photo-instability of Si–C bonds.<sup>49</sup> Kenney and co-workers isolated monoorgano monochloro SiPc derivatives, (RSiPcCl, 10), such as methyl (10a), phenyl (10b) or 3-chloropropyl (10c), by refluxing an alkyl or aryl trichlorosilane (RSiCl<sub>3</sub>) with DII in solvents like quinoline, 2,6-lutidine or 2-picoline and using light-protected synthetic set-ups (Scheme 7).<sup>28</sup> These reactions afforded crude or pure 10 as green solids with yields of ~5–52%. Use of allyl and benzyl trichlorosilanes in these strategies, resulted in formation of only bis-siloxy ether SiPcs, 4 therefore, indicating the limited scope of axial Si–C ligands that can be installed in SiPcs.<sup>63</sup> Symmetrical SiPcs, 11 containing trans-bis Si–C linkages were obtained in high yields (~90%) by refluxing 1 with 2–3 fold excess of Grignard reagents of choice (RMgI) in dry THF for



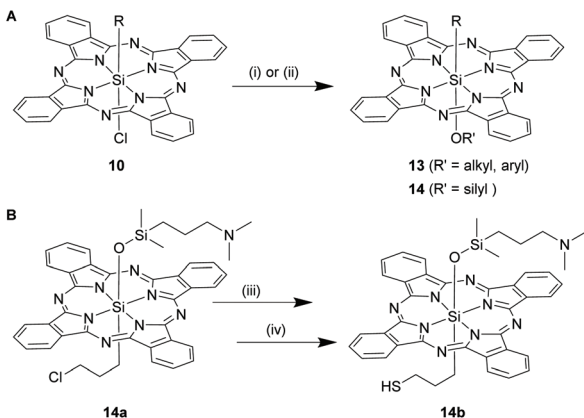
**Scheme 7** Synthesis of axially symmetrical and unsymmetrical Si–C bond containing SiPcs. Reagents and conditions: (i) RSiCl<sub>3</sub>, dry quinoline, reflux, 90 min; (ii) (a) RMgI, dry diethyl ether, N<sub>2</sub>, r.t., overnight, (b) 6 M HCl, 0 °C. R denotes alkyl groups.

several hours under inert and dark conditions (Scheme 7).<sup>49,64</sup> However, only primary alkyl, aryl or alkyne groups (such as methyl, ethyl and phenyl) were successfully inserted using the Grignard reactions. Kumada *et al.* aptly combined the above two strategies and successfully prepared unsymmetrical SiPcs, 12 with direct Si–C bonds in axial positions.<sup>65</sup> They reacted 10 with 6-fold excess of the corresponding Grignard reagent (R' MgI) in dry diethyl ether and stirred at room temperature overnight (Scheme 7). Hydrolysis of the intermediate magnesium adducts was carefully accomplished using aqueous hydrochloric acid at 0 °C. The pure products, 12 were obtained as dark green solids in high yields of ~85%. In contrast to the SiPc analogues with axial Si–O bonds, certain organo SiPcs exhibited better solubility in organic solvents such as chloroform and dichloromethane.

*SiPcs with mixed axial Si–O and Si–C bonds.* The axial chloride of 10 was hydrolysed with concentrated sulfuric acid, followed by addition of ice, to produce monoorgano monohydroxy SiPc derivatives, 13 [R'SiPc(OH)] (Scheme 8A).<sup>28</sup> These hydroxyl derivatives were subsequently refluxed with phenols (e.g. phenol, 4-chlorophenol) in 1,2,4-trimethyl benzene for 30–90 min to yield SiPcs, [R'SiPc(OR)] with trans axial Si–C and Si–O bonds.<sup>28</sup> In a similar fashion, compounds having an axial silyl group, 14 (where R' = silyl) was obtained by directly exposing crude 10 to siloxy ethers (R<sub>3</sub>SiOCH<sub>3</sub>).<sup>22</sup>

Though organo SiPcs were long discovered, appendage of suitable reactive handles in the Si–C bonds was not achieved until recently. Kenney *et al.* synthesized and isolated crude organo SiPc derivative, 10c (R = ClCH<sub>2</sub>CH<sub>2</sub>CH<sub>2</sub> in 10) where the axial Si–C ligand contained a reactive alkyl halide substituent (Scheme 7).<sup>22</sup> Compound 10c was obtained by refluxing equimolar amounts of DII and 3-chloropropyltrichlorosilane





**Scheme 8** Synthesis of axially unsymmetrical SiPcs derivatives containing Si–O and Si–C bonds. Reagents and conditions: (i)  $\text{R}'\text{OH}$ , 1,2,4-trimethyl benzene, 30 min, reflux; (ii)  $\text{CH}_3\text{OSiR}_3$ , chlorobenzene, reflux, 3 h; (iii) potassium thioacetate, dimethylformamide, 50 °C, 6 h; (iv) aqueous sodium hydroxide (2 N), ethanol, 0 °C, 75 min.

in slightly polar solvents like 2,6-lutidine or 2-picoline for 6 h in argon atmosphere (Scheme 7). A similar bromo SiPc derivative was also obtained by using the corresponding bromosilane precursor. However, these compounds could not be purified substantially, presumably owing to their extremely low synthetic yields.<sup>22,66</sup> The displacement the axial Si–Cl bonds of **10a** by a siloxy ether,  $[(\text{CH}_3)_2\text{Si}(\text{OCH}_3)(\text{CH}_2\text{CH}_2\text{CH}_2\text{N}(\text{CH}_3)_2)]$  led to the formation of **14a** which was isolated in yield of ~5% (Scheme 8A). Next, using the chloride group, **14a** was converted to a thiol bearing SiPc, **14b** in two successive steps *via* formation of a thioacetate intermediate (Scheme 8B).<sup>22</sup> The presence of a nucleophilic thiol moiety dangling at the end of the Si–C axial bond created the possibility of functionalization of the organo SiPcs.

The photolabile axial Si–C bonds triggered the development of interesting synthetic routes for the preparation of unsymmetrical SiPcs with axial bis Si–O bonds.<sup>58</sup> For example, compounds **14** ( $\text{R}' = \text{silyl}$ ) on UV or visible light irradiation in trimethylamine saturated water and toluene solvent system at room temperature rendered the hydroxyl SiPc analogues, **6** in high yields which were further derivatized with hydroxyl groups to form SiPcs, **7**.

### 2.3 Synthesis of SiPcs with phthalocyanine ring substitutions

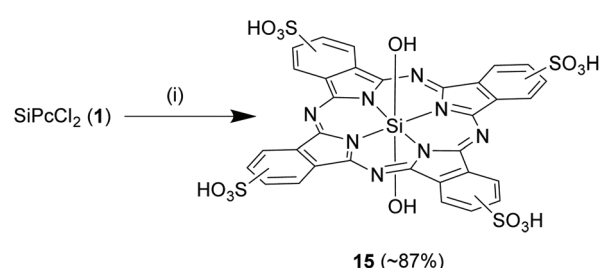
Like axial substitutions, the peripheral rings of SiPcs can be modified at  $\alpha$  and  $\beta$  positions to perturb planarity, reduce aggregation, and increase hydrophilicity or to insert reactive handles for attachment of desired functionalities (Fig. 1C). More importantly,  $\alpha/\beta$  substitutions are exploited to modulate the spectral properties of SiPcs. Various synthetic strategies have been developed for incorporation of halides, alkyl, alkoxy, phenoxy, phenylthio, sulphonate, glycols and vinyl groups at the peripheral and non-peripheral positions and often result in the formation of tetra- or octa-substituted symmetrical SiPcs. A few routes have been also proposed for synthesis of SiPcs with unsymmetrical peripheral substitutions. However,

the latter reactions are synthetically more challenging as they usually result in low synthetic yields and formation of mixtures of products which are difficult to separate.

**2.3.1 SiPcs with symmetrical phthalocyanine ring substitutions.** The  $\alpha/\beta$  decorated symmetrical SiPcs are primarily obtained from three major synthetic approaches: (i) direct reactions of the aromatic rings in SiPc, (ii) initial synthesis of substituted phthalonitrile precursors, followed by conversion to SiPcs *via* the corresponding **DII** derivatives and (iii) initial formation of a substituted Pc ring, followed by direct insertion of the core Si atom. These three strategies are discussed in detail below.

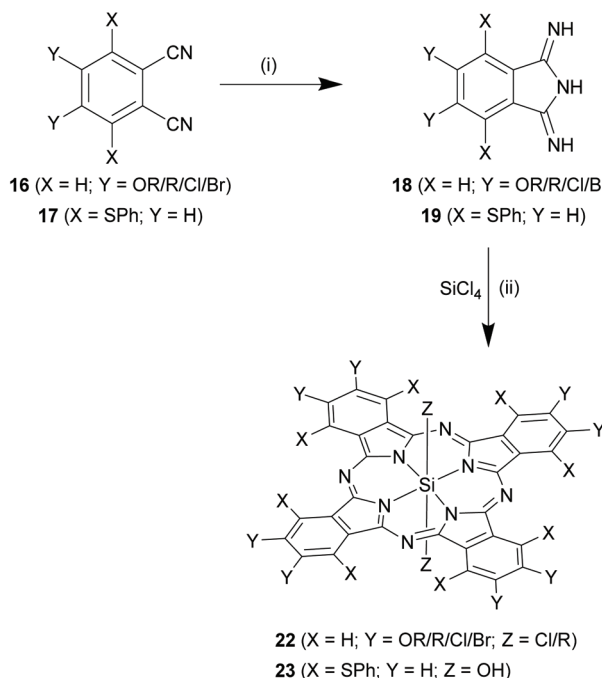
*Direct reaction of the aromatic rings in SiPc.* By means of a direct reaction, the aromatic rings of SiPc can be sulphonated,<sup>66,67</sup> to obtain enhanced photostability as well as aqueous solubility. In a typical reaction, **1** was heated with excess chlorosulphonic acid ( $\text{ClSO}_3\text{H}$ ) at 130 °C for 5 h and then cooled to 85 °C. Thionyl chloride (30-fold excess) was slowly added to the solution and the reaction was continued for another 4 h. The resulting sulphonyl chloride SiPc adduct was isolated in pure form (yield ~68%) and then hydrolysed in methanol–water (1 : 5 v/v mixture) under reflux conditions for 3 h to obtain the tetrasulphonated SiPc, **15** in high reaction yields of ~87% (Scheme 9).<sup>67</sup> Importantly, the varying degrees of sulphonation depend on the SiPc :  $\text{ClSO}_3\text{H}$  molar ratio and thus can be controlled. For example, use of SiPc and  $\text{ClSO}_3\text{H}$  in 1 : 4 molar ratio resulted in isomeric mixtures of  $\alpha$  or  $\beta$  substituted (Fig. 1) monosulphonated unsymmetrical SiPcs.<sup>66</sup>

*Using substituted phthalonitriles as precursors.* The choice of substituted phthalonitriles, **16** or **17** as precursors varied according to the nature and position of the desired substituents (Scheme 10). For synthesis of symmetrical  $\beta$ ,  $\beta$  substituted SiPcs (**22**, where  $\text{X} = \text{H}$ ), 4,5-disubstituted phthalonitriles (**16**, where  $\text{X} = \text{H}$ ) were used as precursors. Depending on the nature of  $\text{Y}$  groups, compounds **16** were synthesized from either 4,5-dibromo catechol or 4,5-dichloro dicyanobenzene. The subsequent steps for formation of SiPcs, **22** were common in both the cases and proceeded *via* the formation of the corresponding **DII** derivatives, **18** (Scheme 10). In some cases, purification of the SiPc chloro analogues were difficult and required further transformation of the axial chloro group to a hydroxyl or siloxy group.



**Scheme 9** Sulphonation reaction of the aromatic rings of SiPc. Reagents and conditions: (a) chlorosulphonic acid, 130 °C, 5 h, (b) thionyl chloride, 4 h, (c) methanol–water (1 : 5 v/v), reflux, 3 h.





**Scheme 10** Synthesis of SiPc derivatives symmetrically substituted at the  $\alpha$  or  $\beta$  positions by using DII derivatives. Reagents and conditions: (i) Na, liq  $NH_3$ , diglyme or (a)  $NH_3$  gas,  $NaOCH_3$ , methanol, 40 min, r.t.; (b) reflux, 3.2 h; (ii)  $SiCl_4$ , dry quinoline, reflux (180–219 °C), 0.5–24 h. X and Y denote different functional groups.

Diether dicyano phthalonitriles (**16a**, where  $X = H$  and  $Y = OR$ ) were obtained from 4,5-dibromo catechol by initial base mediated nucleophilic reaction of the hydroxyl groups and subsequent conversion of the bromides to cyanides *via* Rosemund-von Braun reaction. Lieberman *et al.* used this approach to obtain a crude product mixture containing octa-pentyloxy SiPc derivatives, **22a** ( $X = H$ ;  $Y = pentyloxy$ ;  $Z = Cl$  in **22**) *via* the DII derivative **18a**.<sup>63</sup> A similar approach was also adopted to obtain pentyloxy groups in the peripheral positions of SiPc (yield ~45%).<sup>49</sup>

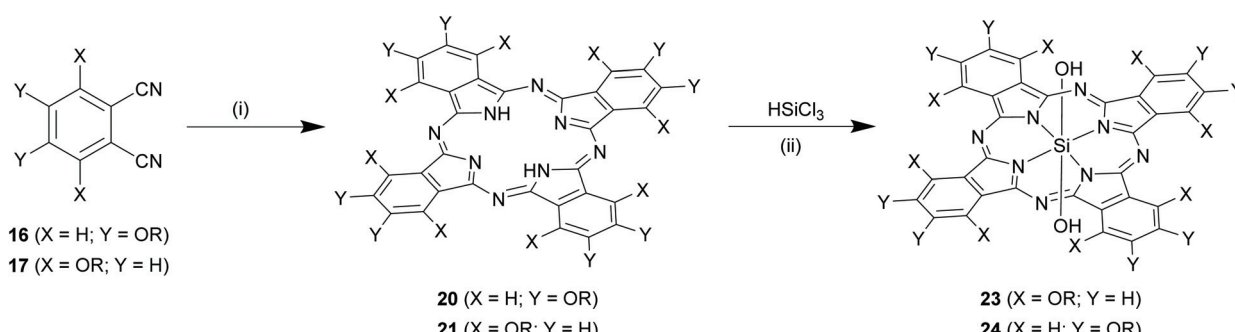
The other route involved 4,5-dichloro dicyanobenzene as the starting material. The two chloro groups were readily sub-

stituted with nucleophiles in presence of a base in polar solvents such as DMF and DMSO and afforded phthalonitriles, **16** (where  $X = H$ ) in a single step reaction. This approach has been utilized for the synthesis of SiPc variants bearing phenoxy (~yield ~67%),<sup>15</sup> and thioalkoxy as peripheral groups.<sup>68</sup> In another report, 4,5-dihalo dicyanobenzenes ( $Y = Cl/Br$ ), as such, was converted to phthalonitriles, **16b** and further reacted to form DII **18b** and insert halogens in the peripheral positions of SiPcs, **22b** (where  $X = H$ ,  $Y = Cl/Br$ ;  $Z = Cl$  in **22**; yields ~72–80%).<sup>31</sup>

In another example, eight peripheral pentyl groups were incorporated in a SiPc structure (**22c**, where  $X = H$ ;  $Y = \text{pentyl}$ ;  $Z = CH_3$  in **22**) using 1,2-dichlorobenzene as the starting material.<sup>49</sup> In the first step, Grignard coupling of 1,2-dichlorobenzene with pentylbromomagnesium was performed to obtain the 1,2-dipentyl benzene. This product was initially subjected to bromination and next, the aromatic bromides were converted to cyanides using  $CuCN$ . Finally, the resulting phthalonitrile **16c** was converted into DII derivative, **18c** and subsequently to **22c** with a reaction yield of ~42%.<sup>49</sup> Similarly, use of naphthalonitrile (2,3-naphthalenedicarbonitrile) instead of a phthalonitrile, generated silicon naphthalocyanines (SiNcs) with a reaction yield of ~82%.<sup>6</sup> The SiNcs, a subclass of SiPcs, absorb and emit in the NIR region owing to the extended  $\pi$ -conjugation of the aromatic rings.

SiPcs bearing  $\alpha,\alpha$  substituents (**23**, where  $Y = H$  in Scheme 10) were generated through the use of 3,6-disubstituted phthalonitriles (**17**, where  $Y = H$ ). One such example has been reported by Nakagawa and co-workers.<sup>69</sup> The synthesis involved prior conversion of 3,6-hydroxyphthalonitrile to 3,6-(bisphenylthio)phthalonitrile *via* tosylation of the hydroxyl groups and base-mediated displacement by thiophenol. The phthalonitrile **17**, thus obtained was first converted to corresponding DII derivative, **19** and eventually to  $\alpha,\alpha$ -octaphenylthio SiPc derivative, **23a** ( $X = phenylthio$ ;  $Y = H$ ;  $Z = OH$  in **23**; yield ~84%).

*Direct insertion of the core silicon to a pre-formed Pcs.* A more flexible synthetic methodology to form SiPc variants at  $\alpha/\beta$  positions involved initial formation of core element-free Pcs, followed by insertion of core silicon atom (Scheme 11).<sup>70</sup> In a



**Scheme 11** Synthesis of symmetrical SiPc derivatives by direct insertion. Reagents and conditions: (i) Lithium carbonate, 1-pentanol, reflux, 66 h or 1,8-diazabicyclo[5.4.0]undec-7-ene (DBU), reflux, 48 h; (ii) (a)  $HSiCl_3$ , DBU, dichloromethane, argon, r.t., 80 min, (b)  $H_2O$ , r.t. X and Y denote different functional groups.

typical reaction, phthalonitriles (**16** or **17**) were refluxed with lithium carbonate (~4-fold excess) in 1-pentanol for 66 h to obtain Pcs (**20** or **21**) in ~30% reaction yields.<sup>71</sup> This conversion proceeded faster (~48 h) and efficiently (high reaction yields ~55–72%) in presence of non-nucleophilic strong bases like 1,8-diazabicyclo[5.4.0]undec-7-ene (DBU).<sup>68</sup> In the final step, these Pcs (**20** and **21**) were reacted with 10–30-folds excess of trichlorosilane ( $\text{HSiCl}_3$ ) to form the desired SiPcs with symmetrical  $\alpha/\beta$  substituents and hydroxyl axial ligands, **23** and **24** (Scheme 11). Reactions were conventionally carried out in anhydrous and inert atmosphere using organic solvents such as DCM, tetrahydrofuran, acetonitrile or toluene at room temperature or under reflux conditions.<sup>70</sup> The nature of the base (such as tripropylamine, tributylamine and DBU) employed affected both reaction completion times and yields (~12–53%) of desired SiPcs (**23** or **24**).<sup>72,73</sup>

**2.3.2 SiPcs with unsymmetrical phthalocyanine ring substitutions.** Mono or di-substituted unsymmetrical SiPcs are synthesized either directly by condensing two different phthalonitriles or indirectly by initial conversion of these phthalonitriles to the corresponding DII derivatives followed by condensation. In the former strategy, an unsymmetrical Pc is first obtained which is then subjected to direct insertion method to insert a silicon atom in the unsymmetrical Pc core. In almost all the cases, the axial chlorides were replaced by hydroxyl or siloxy groups for successful isolation of the peripherally unsymmetrical SiPcs in pure form. The final reaction yields of pure SiPcs varied from 3–27%. This technique led to the synthesis and isolation of SiPcs bearing a reactive handle only in one of the four benzene rings (Fig. 2). This enabled incorporation of functional groups at the periphery and led to the development of SiPc molecules with remarkable biological properties.<sup>43,74,75</sup>

In conclusion to this section, all the aforementioned strategies provided diverse reaction schemes to fabricate SiPcs with ligands of choice such as acidic, basic, neutral, hydrophilic, lipophilic, electron rich or electron withdrawing substituents. This led to exploration and exploitation of the NIR optical properties of SiPc in various contexts.

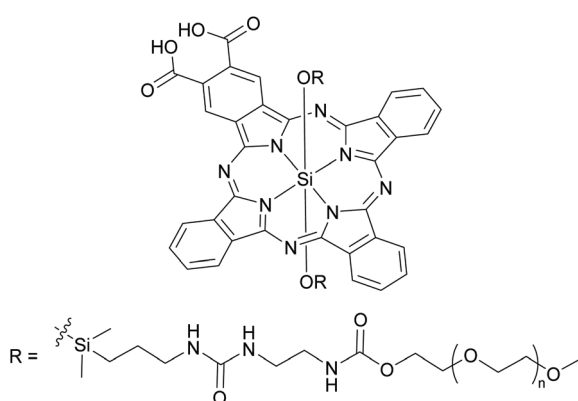


Fig. 2 Chemical structure of a SiPc polymeric derivative, La Jolla Blue with unsymmetrical peripheral ( $\beta$ ) substitutions.

### 3. Applications of silicon phthalocyanines

SiPc derivatives display interesting optical, redox, electronic properties and high thermal stability. In addition, availability of multiple synthetic strategies have resulted in enormous flexibility of SiPc frameworks. Easy modulation of solubility, optical and redox properties, bio-compatibility, bioactivity or solid-state structural arrangements has been achieved through decorating both axial and peripheral positions. This led to a multitudinous array of SiPc derivatives that have been crafted according to the demands for particular applications. The past decade has experienced an upsurge of novel applications of SiPcs in medicinal chemistry, photovoltaics, optoelectronics and photocatalysis. Selected examples of these emerging applications are discussed below.

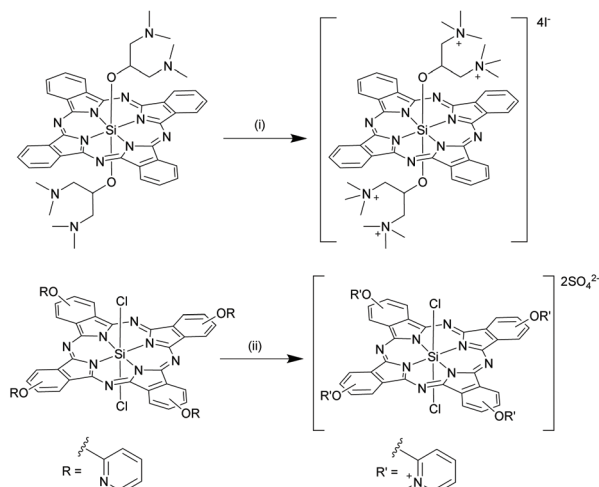
#### 3.1 Applications of SiPcs in medicinal chemistry

Silicon phthalocyanines have been extensively pursued in light-based medical applications, primarily as anticancer, antibacterial and antifungal agents.<sup>23,76–78</sup> Owing to the strong NIR emission, SiPcs have been potentially applied for *in vitro* and *in vivo* bioimaging.<sup>32,52,79–81</sup> Two fluorescent SiPc derivatives, namely La Jolla Blue® and IRD700DX®, are commercially available as labelling agents for biomolecules.<sup>82–84</sup> Likewise, due to the intense far red and NIR Q-band absorptions, several photosensitive SiPc molecules have been deployed in photodynamic therapy (PDT), photouncaging techniques, photoimmunotherapy (PIT), and photothermal therapy (PTT). A few recent noteworthy examples are highlighted in the subsequent sections.

**3.1.1 Incorporation water soluble axial or peripheral ligands.** The most sought after modification of SiPcs has been to reduce aggregation tendencies and overcome the stunted solubility, a factor that restrains the biological applications of most Pcs. One extensive methodology pursued to improve the aqueous solubility is the incorporation of nitrogen rich substituents in the axial or peripheral positions of SiPcs, which can be readily alkylated to give quaternary ammonium salts using methyl iodide, dimethyl sulfate or 1,3-propanedisulfone to obtain cationic water soluble SiPc derivatives, mostly suitable for biological applications (Scheme 12).<sup>15,17,19,33,59,69,85,86</sup>

**3.1.2 SiPcs in photodynamic therapy (PDT) of cancer.** Photodynamic therapy is a minimally-invasive anticancer modality which typically involves a local or systemic administration of a photosensitizer followed by activation in the cancerous tissues with light irradiation.<sup>87,88</sup> SiPc based compounds are second generation photosensitizers which display moderate to high quantum yields of NIR light induced generation of singlet oxygen, a short-lived and highly cytotoxic species. The promising activity of Pc-4 (**6**) in clinical trials<sup>89</sup> has sparked renewed interest in researchers to improve efficacy of Pc-4.<sup>90–94</sup> In parallel, several approaches were adopted to increase the aqueous solubility and biocompatibility leading to development of new SiPc photosensitizers. For example, a





**Scheme 12** Synthesis of water soluble SiPc derivatives. Reagents and conditions: (i) Methyl iodide, chloroform, reflux, 85 °C, 6 h; (ii) dimethyl sulphate, dimethylformamide, 120 °C; 24 h.

SiPc derivative with two bulky permethylated cyclodextrin moieties in the axial positions displayed reduced self-aggregation in the cell culture media and remarkable *in vitro* and *in vivo* PDT effects.<sup>38</sup> Likewise, SiPcs conjugated axially with biomolecules such as nucleosides<sup>95</sup> and serum albumin<sup>96</sup> exhibited enhanced cellular uptake. Furthermore, incorporation of tumor targeting moieties such as erlotinib,<sup>97</sup> hyaluronic acid,<sup>52</sup> and biotin<sup>98</sup> in the SiPc framework resulted in excellent tumor specific uptake and PDT effects. In other approaches, SiPc molecules have been covalently linked with chemotherapeutic drugs to generate chemo-photodynamic conjugates having dual mode of cytotoxic action.<sup>19,32,52,99</sup>

Recently, You's research group developed SiPc pseudoprodrugs to execute multipurpose objectives such as (i) fluorescence imaging, (ii) far red light-mediated uncaging, and (iii) combined effects of singlet-oxygen induced PDT and local chemotherapy.<sup>100–103</sup> They utilized singlet oxygen-labile aminoacrylate bonds to append clinical chemotherapeutic drugs such as combretastatin and paclitaxel in the axial positions of SiPcs (**3b** and **3c** in Fig. 3A).<sup>101,103</sup> The caged forms **3b** and **3c** exhibited significantly reduced dark cytotoxicity as evident from 19 and 190-folds lower IC<sub>50</sub> values when compared to the respective free drugs. On light irradiation, SiPc produced singlet oxygen which led to an immediate PDT effect and simultaneously cleaved the aminoacrylate linker to uncage the intact chemotherapeutic drugs. This bystander or local chemotherapeutic effect after the illumination was demonstrated by exposing only one-half of each well containing cancer cells treated with vehicle only, **3b** or a structurally equivalent non-photocleavable SiPc conjugate, NCL-**3b** (Fig. 3B). The PDT effect of NCL-**3b** was restricted only in the light exposed half of the well due to the short half-life (10–320 ns) and limited diffusion distance (20–200 nm) of singlet oxygen (panel (c) of Fig. 3B).<sup>88</sup> However, the **3b**-treated wells showed prominent bystander effects. The photoreleased combretastatin diffused

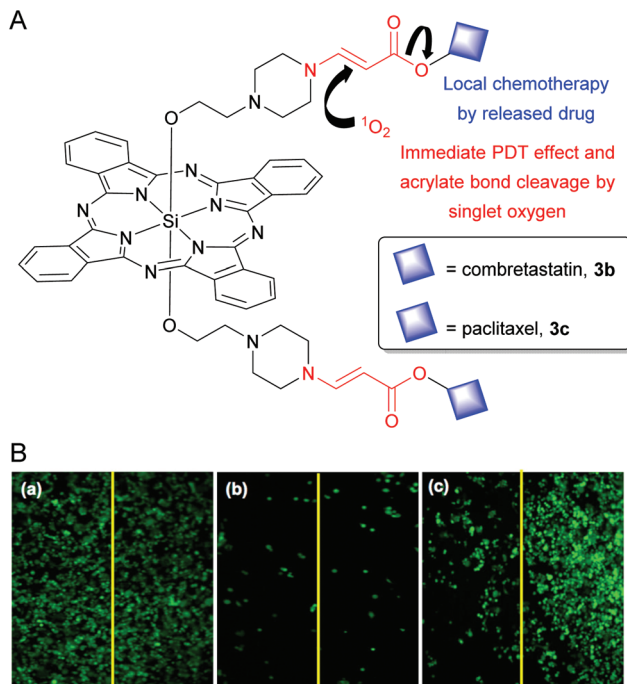


**Fig. 3** (A) Structure of SiPc **3b** and **3c** showing dual PDT and singlet oxygen mediated release of chemotherapeutic drug (shown as blue squares). (B) Fluorescence live cell images of the center of each well treated with (a) vehicle control, (b) 25 nM **3b**, and (c) 25 nM NCL-**3b**. The left half of each well was illuminated with a 690 nm diode laser (11 mW cm<sup>-2</sup> for 15 min). At these concentrations, **3b** and NCL-**3b** did not produce any significant dark toxicity. Reproduced with permission from ref. 101. Further permissions related to the material excerpted should be directed to the ACS (<https://pubs.acs.org/doi/10.1021/jm5000722>).

throughout the well and caused similar toxicity in the light unexposed cells as compared to light-exposed cells (panel (b) of Fig. 3B).

Compound **3b** was further modified to incorporate a tumor-targeting folic acid at the second axial position *via* a hydrophilic PEG linker.<sup>102</sup> It was observed that the longer length of the PEG spacer enhanced specific uptake and localization in folate receptor overexpressing colon 26 tumors. The SiPc conjugate having PEG linker length of ~45 showed the most impressive light induced cytotoxicity giving a IC<sub>50</sub> value of 1.65 × 10<sup>-8</sup> M (690 nm, 10 J cm<sup>-2</sup>), while being non-toxic in the dark at <2 μM concentration.

**3.1.3 NIR dissociation of axial ligands of SiPcs.** An interesting feature of SiPc is the photolability of unique axial Si–C and Si–O bonds.<sup>20,63</sup> Though this photochemical degradation of SiPcs was long-established, it has been only recently exploited in medicinal chemistry to photorelease PDT and chemotherapeutic anticancer agents selectively in a cancer microenvironment.

**3.1.4 SiPcs as photocages.** Burda *et al.* utilized the photo-sensitive Si–C axial bond for NIR light-controlled delivery of Pc-4.<sup>21</sup> They judiciously chose PEGylated gold nanoparticles (Au NPs) as drug-delivery systems due to their excellent biocompatibility and superior drug loading capacity. Facile syn-

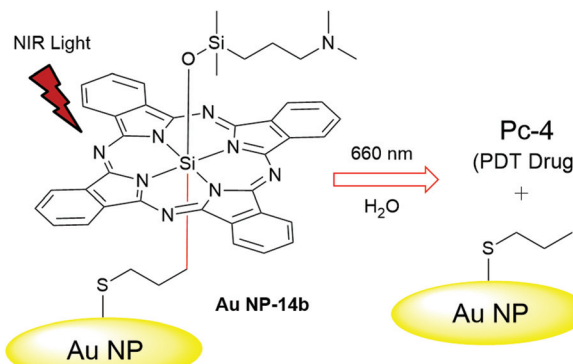


**Fig. 4** Schematic representation of phototriggered PDT drug **Pc-4** release from **Au NP-14b**. The thiol group in **14b** allowed covalent bonding of the drug precursor to the Au NP surface. Adapted from ref. 21 with permission. © 2014 WILEY-VCH Verlag GmbH & Co. KGaA, Weinheim.

thesis of stable covalent assemblies of SiPc and AuNP, **Au NP-14b** was executed by taking advantage of the thiophilic nature of gold and the free thiol group of **14b**. On red light exposure, the Si-C bond in PEGylated **Au NP-14b** rapidly dissociated to release **Pc-4** molecules (Fig. 4). Interestingly, the drug can only be photo-released in lipophilic environments. The Au NPs displayed only ~1% cellular uptake and insignificant cellular toxicity. Therefore, as expected, **Au NP-14b** conjugates caused no change in viability of HeLa (cervical cancer) cells in the dark. In contrast, almost 80% of the population were killed in **Au NP-14b** (1  $\mu$ M) treated HeLa cells which were illuminated (>600 nm, 1 J  $\text{cm}^{-2}$ , 12 min). This toxicity profile was comparable to that of unformulated **Pc-4**, thereby suggesting the photorelease of **Pc-4** from the nanoparticle conjugates.

The research groups of Kenney and Burda performed theoretical and experimental measurements to identify the preferred mechanistic pathway of the light triggered Si-C bond cleavage process.<sup>22,104,105</sup> Characterization of the photo-products using various techniques such as steady state spectroscopy, electrospray ionization mass spectrometry, liquid chromatography mass spectrometry, nuclear magnetic resonance and electron paramagnetic resonance hinted towards formation of a relatively long-lived SiPc radical as the key intermediate which consequently undergoes solvolysis.<sup>104</sup> Computational studies additionally confirmed homolytic bond cleavage process involving radical intermediates. Bond-dissociation energy (BDE) calculations indicated that homolytic cleavage (~50 kcal  $\text{mol}^{-1}$ ) is energetically more favoured than heterolytic cleavage (~190 kcal  $\text{mol}^{-1}$ ).<sup>22</sup> This is due to the fact that the unpaired electron is largely delocalized over the SiPc aromatic rings as implied by natural bond orbital (NBO) analysis and spin density calculations.

In another recent report, Schnermann *et al.* demonstrated the preferential photocleavage of Si-O bonds and release of phenols in axially unsymmetrical SiPcs molecules.<sup>19</sup> On NIR photoexposure at the SiPc Q-band (690 nm), the axial Si-O bonds in **8d** and **8e** (Scheme 5, above) instantly dissociated in

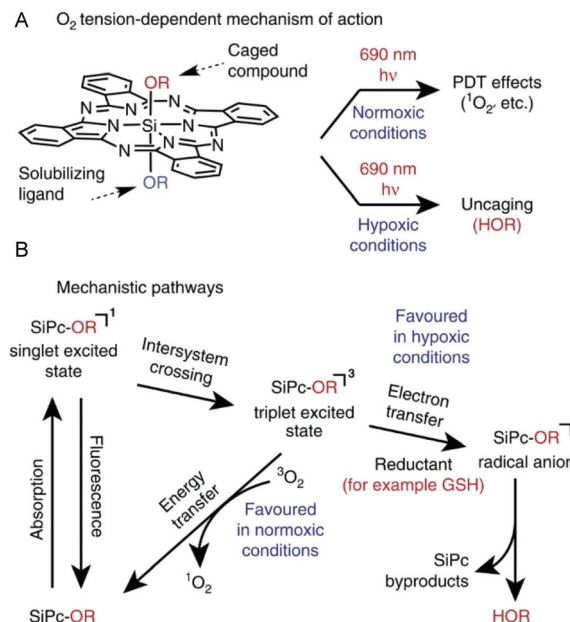


**Fig. 5** (A)  $\text{O}_2$  tension dependent mechanism of action of SiPc. (B) Mechanistic pathways leading to ROS generation or small molecule uncaging. R denotes aryl group. Reproduced from ref. 19.

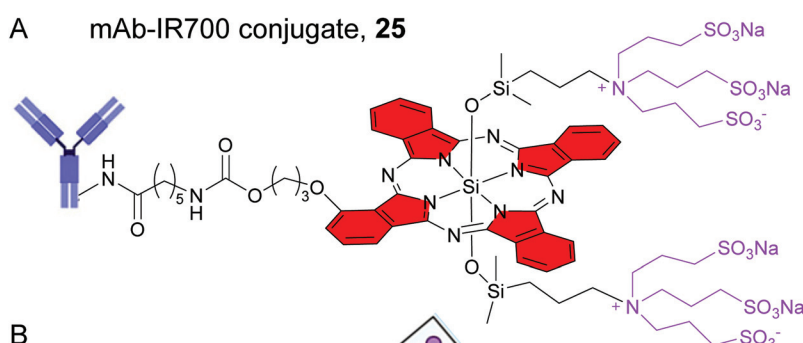
oxygen-deprived physiological conditions and in presence of reducing glutathione (GSH, 5 mM). Thus, photo uncaging of small phenolic molecules such as fluorescent 4-methyl umbelliflione or clinical anticancer drug combretastatin was achieved (Fig. 5A). In contrast, compounds **8d** and **8e** were fairly stable on light irradiation under normoxic conditions and produced singlet oxygen as the major reactive oxygen species (Fig. 5A). Thus, compound **8e** resulted in NIR mediated cytotoxicity in cancer cells which was a manifestation of either PDT or chemotherapy depending on the availability of tissue oxygen. Compound **8e** (200 nM) showed NIR (690 nm, 50 J  $\text{cm}^{-2}$ ) induced phototoxicity by a PDT mechanism in presence of oxygen leading to 48% cell growth inhibition. In hypoxic conditions, the cell growth inhibition increased to 80% which is comparable to that of free combretastatin suggesting photo-release of the chemotherapeutic agent from the SiPc molecule triggered by NIR light and cytosolic glutathione (Fig. 5A).

Detailed spectroscopic and computational studies were performed to understand the photoredox uncaging reactions.<sup>106</sup> The proposed mechanistic pathway involved a key radical anion intermediate formed through photoinduced electron transfer from the SiPc triplet state (Fig. 5B). This explained the role of reducing agent, glutathione in accelerating the cleavage phenomenon. The transient radical anion was proposed to undergo solvolytic ligand exchange through a heptacoordinate silicon transition state.

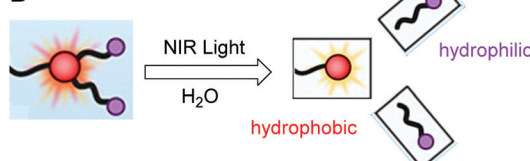
**3.1.5 SiPcs in photoimmunotherapy.** In their seminal paper, Kobayashi and co-workers employed monoclonal antibody-SiPc conjugates, mAb-IR700 (**25**) in photoimmunotherapy (PIT), a novel molecular-targeted cancer modality that combines PDT and immunotherapy (Fig. 6A).<sup>80</sup> The conjugates



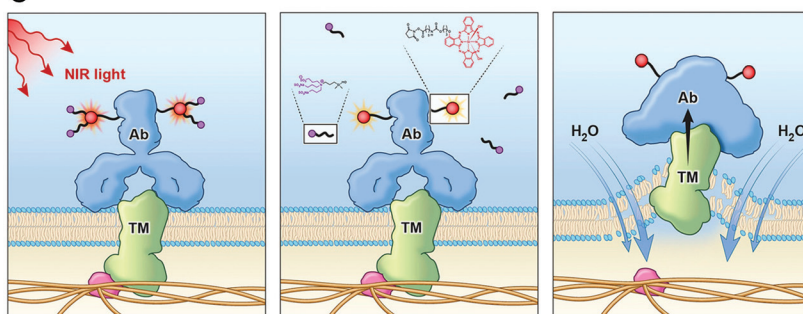
## A mAb-IR700 conjugate, 25



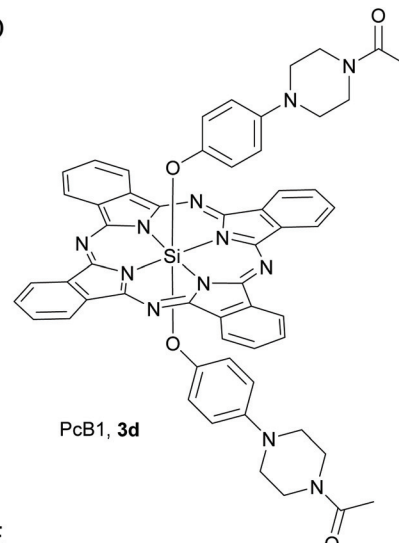
B



C



## D



E

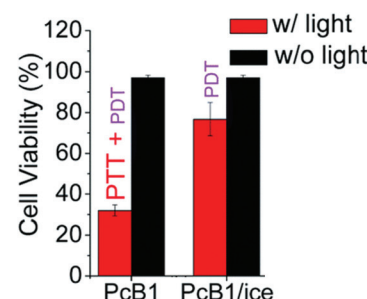


**Fig. 6** (A) Structure of mAb-IR700 conjugate, 25. The red colour is used to highlight hydrophobic SiPc core rings and the violet colour is used to highlight the hydrophilic axial ligands. (B) NIR light induced decomposition of the SiPc molecule attached to the antibody. NIR light irradiation causes mAb-IR700 to release the hydrophilic ligand (violet circles), which makes mAb-IR700 hydrophobic and causes aggregation. (C) Scheme indicates the proposed mechanism of NIR-PIT. An antibody-IR700-antigen complex is formed on the cell membrane. With NIR light irradiation, the ligands of IR700 were released from the antibody-IR700-antigen complex. The physical changes in aggregation and solubility of the antibody-IR700-antigen complex may produce physical stress on the membrane locally impairing cellular membrane function for maintaining membrane pressure, and then the water outside of the cell was flown into the cell to burst the cell. Reproduced with permission from ref. 18. Further permissions related to the material excerpted should be directed to the ACS (<https://pubs.acs.org/doi/10.1021/acscentsci.8b00565>). (D) Chemical structure of SiPc, 3d or Pcb1. (E) Cytotoxic effect of 3d or Pcb1 on HepG2 cells with (red bars) and without (black bars) laser irradiation. Pcb1/ice mean controlling the temperature of cells at below 30 °C via an ice-bath during laser treatment. Reproduced from ref. 110 with permissions from Royal Society of Chemistry.

25 comprised of a cell-impermeable, hydrophilic, NIR absorbing SiPc photosensitizer (IR700 dye) which was covalently tethered to monoclonal antibodies targeting human epidermal growth factor receptors (HER or EGFR). It is important to note that one such SiPc derivative, where IR700 is conjugated to cetuximab, recently gained approval as a NIR PIT drug by the Japanese government for treatment of head and neck cancers.<sup>107</sup> The cell membrane-bound conjugates 25 showed tumor-specific cytotoxicity in HER expressing tumor xenografts only when exposed to NIR light. Interestingly, unlike PDT, internalization of the photosensitizer was not required in PIT and the light induced cytotoxicity was only partially derived from reactive oxygen species. In another report, Mitsunaga *et al.* combined an antibody (Trastuzumab, T), a chemotherapeutic drug (maytansinoid, DM1) and NIR absorbing SiPc photosensitizer (IR700) to generate bifunctional antibody-drug-photoabsorber conjugates (T-DM1-IR700).<sup>108</sup> *In vivo*

studies with these conjugates showed HER-2 targeted tumor cytotoxicity *via* dual action NIR-PIT and chemoimmunotherapy. Remarkably, T-DM1-IR700 conjugates exhibited cytotoxicity in deep-seated tumors where NIR-PIT by itself fails due to insufficient NIR light penetration.

Recently, Kobayashi and co-workers unravelled the distinct mechanism of PIT for SiPc-antibody conjugates. They observed NIR light induced dissociation of the axial Si-O-Si linkages in 25 in presence of an electron donor such as ascorbic acid sodium salt, NaAA (Fig. 6B).<sup>18,109</sup> The NIR light triggered detachment of hydrophilic sulphonated axial ligands led to an increase in hydrophobicity of 25 and consequently resulted in aggregate formation and quenching of NIR fluorescence. Atomic force microscopy (AFM) revealed alteration in the protein conformation such as enlargement of the conjugates and loss of normal Y-shape of the antibody. Thus, the photoinduced degradation not only affected the physical



shape and solubility of the covalently-conjugated antibody, but also influenced the antibody-antigen complexes. These profound morphological changes were speculated to enhance the transmembrane (TM) water flow which created physical stress within the cellular membrane and eventually led to cell bursting and necrotic/immunogenic cell death (ICD) (Fig. 6C).

**3.1.6 SiPc in photothermal therapy.** Photothermal therapy (PTT) is an oxygen-independent anticancer treatment in which appropriate light energy is absorbed by photosensitive molecules and converted into thermal energy, ultimately leading to hyperthermia mediated cancer cell death.<sup>87</sup> Huang and co-workers designed a SiPc derivative, PCB1 or **3d** and studied its photothermal behaviour (Fig. 6D).<sup>110</sup> The two nitrogen-rich axial substituents effectively fostered photoinduced electron transfer (PET) mechanism and lowered the fluorescence and singlet oxygen generation quantum yields of SiPc, **3d**. Temperature escalated by 28 °C on laser irradiation (730 nm) of aqueous solutions of **3d**. However, such photothermal characteristics were lost upon protonation of the axial ligands highlighting the crucial roles of nitrogen lone pairs in the PET process. NIR exposure of **3d**-treated human liver cancer cells (HepG2) led to ~70% decrease in cell viability indicating its ability to act as a unique PTT agent (Fig. 6E). Similar viability assays performed under ice-bath conditions showed only ~30% loss in cell viability which might be attributed to the PDT effect of **3d** (Fig. 6E).

### 3.2 Applications in organic photovoltaic solar cells

SiPcs have recently generated interest for multifunctional applications in dye-sensitized (DSSCs), bulk heterojunction (BHJ) and planar heterojunction (PHJ) solar cells as additives, acceptors, donors and crosslinking components.<sup>111</sup> The intense absorption of chemically and thermally robust SiPcs and SiNcs in the red and far-red spectral region has been utilized to expand the light harvesting window and boost the overall photoconversion efficiency (PCE). The structural tunability has led to easy integration and multi-functional behaviour. Finally, the low toxicity levels and the elemental abundance of silicon in nature have particularly advocated for their candidacy in organic photovoltaics and optoelectronics.

**3.2.1 SiPc as additives in solar cells.** Honda *et al.* pioneered the use of a bis(*tri-n*-hexylsilyl oxide) substituted SiPc derivative, **4b** as an ternary additive in a P3HT/PCMB [(poly(3-hexylthiophene)/(phenyl-C<sub>61</sub>-butyric acid methyl ester))] BHJ solar cell and observed a positive influence of the dye in overall device performance (Fig. 7).<sup>112</sup> The values for short-circuit current (*J<sub>sc</sub>*), open-circuit voltage (*V<sub>oc</sub>*) and the fill factor (FF) of 10.3 mA cm<sup>-2</sup>, 0.57 V and 0.69 respectively were achieved at optimized loading content of 4.8 wt% for **4b** (Table 1, Fig. 7). The presence of the dye boosted PCE to 4.1. Transient absorption spectroscopy and surface energy measurements revealed the presence of a cascaded photoconversion mechanism in which facile charge transfer occurred from P3HT to PCBM *via* SiPc molecules aided by their intermediate energy levels and selective localization in a disordered P3HT domain and at the polymer-fullerene interface.<sup>112-114</sup> Hence, the overall device

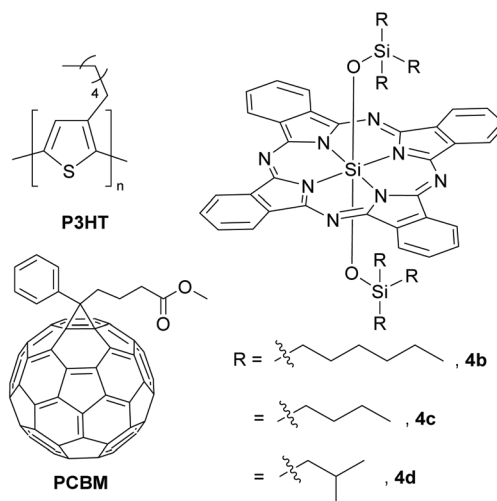


Fig. 7 Chemical structures of P3HT, PCBM and SiPc derivatives **4a–4c**.

performance was governed by the blend morphology which in turn depended on both dye structure and dye loading content.

Encouraged by these inferences, Bender and co-workers varied the alkyl spacer of the axial silyl groups of dye **4b** and observed that use of smaller molecular fragments such as *tri-n*-butyl silyl (**4c**) and *tri-isopropyl* silyl (**4d**) in the axial positions led to ~10% increase in *J<sub>sc</sub>* values when compared to **4b** (Fig. 7, Table 1).<sup>40</sup> These experimental outcomes led to the conclusion that the SiPc dyes with contrasting properties of high solubility and extreme tendency to crystallize favoured charge transfer and augmented the overall device efficiency. A more rigorous study using eight SiPc variants with axial alkylsilyl groups of different chain lengths has been recently reported.<sup>44</sup> It was observed that SiPc variants displayed similar optical, electrochemical and hydrophobicity properties and frontier orbital energy levels. However, the alkyl chain length had a pronounced effect in molecular packing and solubility of the SiPc dyes and thus governed the overall device performance. Best PCE values were achieved in cases where solubility of the ternary additive SiPc dye matched closely to that of P3HT.

In parallel, researchers explored SiPc structural variants with axial functionalities other than siloxy ethers, such as alkyl/aryl ethers and esters, as alternate additives in BHJ solar cells. Bender and co-workers investigated the device performance of bis(3-pentadecylphenoxy)-SiPc, **3e** (Fig. 8).<sup>30</sup> Albeit having similar spectral features like **4b**, the dye **3e** failed to significantly increase the *J<sub>sc</sub>* and the efficiency (*η<sub>eff</sub>*) of the polymer-fullerene based ternary cascade BHJ solar cell (Table 1). Compound **3e** exhibited lower tendencies to crystallize and migrate to the P3HT/PCBM interface as compared to **4a**. The authors speculated that these factors might be responsible for its inferior performance.

In another approach, Ameri *et al.* synthesized SiPc derivatives with bulky *t*-butyl groups in the periphery and flexible axial pyrene carboxylic acid groups to fabricate ternary BHJ



**Table 1** The performances and device characteristics of photovoltaic devices containing various SiPc and SiPc derivatives as additives, donor or acceptor materials

Type of solar cell	Donor/acceptor pair	Additive dye(s)	Loading (wt%)	$J_{SC}$ /mA cm <sup>-2</sup>	$V_{OC}$ /V	FF	PCE (%)	Ref.
BHJ	P3HT/PCBM	—	—	8.48	0.57	0.56	2.74	30
BHJ	P3HT/PCBM	<b>4b</b>	4.8	10.3	0.57	0.69	4.1	112
BHJ	P3HT/PCBM	<b>4b</b>	3.7	9.84	0.57	0.59	3.29	30
BHJ	P3HT/PCBM	<b>4c</b>	3.7	10.0	0.56	0.59	3.30	40
BHJ	P3HT/PCBM	<b>4d</b>	3.7	10.1	0.57	0.60	3.40	40
BHJ	P3HT/PCBM	<b>3e</b>	3.7	9.49	0.59	0.54	3.02	30
BHJ	P3HT/PCBM	<b>5a</b>	20	10.02	0.65	0.63	4.14	115
BHJ	P3HT/PCBM	<b>26</b>	8	11.4	0.62	0.63	4.46	116
BHJ	P3HT/PCBM	<b>4b/27</b>	4.8/1.5	10.9	0.57	0.69	4.3	112
BHJ	P3HT/PCBM	<b>5b/28</b>	7.5/5	10.80	0.65	0.55	3.89	117
BHJ	P3HT/PCBM	<b>28</b>	10	9.72	0.65	0.58	3.68	117
DSSC	—	<b>29</b>	—	19.0	0.46	0.51	4.5	118
BHJ	P3HT/ <b>4b</b>	—	—	0.99	0.70	0.37	0.25	40
BHJ	P3HT/ <b>4c</b>	—	—	2.61	0.75	0.40	0.78	40
BHJ	P3HT/ <b>4d</b>	—	—	3.0	0.84	0.43	1.07	40
PHJ	<b>1/C<sub>60</sub></b>	—	—	0.47	0.24	0.32	0.04	36
PHJ	<b>3f/C<sub>60</sub></b>	—	—	1.4	0.76	0.31	0.34	36
PHJ	<b>3g/C<sub>60</sub></b>	—	—	4.6	0.87	0.44	1.8	119
PHJ	$\alpha$ -6 T/ <b>3h</b>	—	—	3.5	0.66	0.43	1.0	119
BHJ	PTB7/ <b>5c</b>	—	—	0.60	1.00	0.45	0.27	120
BHJ	PTB7/ <b>5d</b>	—	—	6.18	1.03	0.42	2.67	120

$C_{60}$  is fullerene.  $\alpha$ -6 T is  $\alpha$ -sexithiophene. PTB7 is an organic semiconducting polymer. All values are taken from the references as listed in the last column.

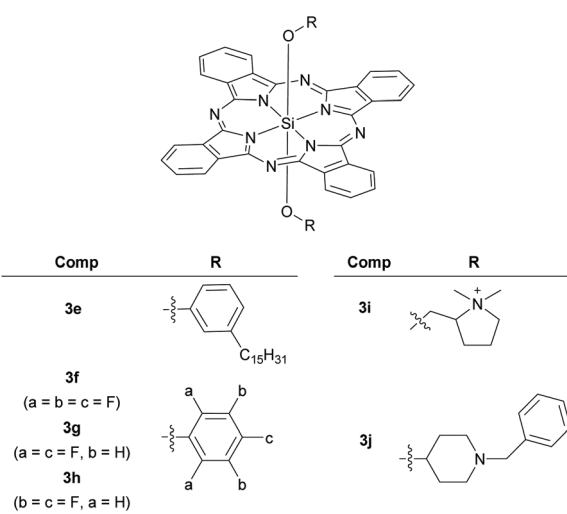


**Fig. 8** Chemical structures of SiPc derivatives, **3e**–**3j**.

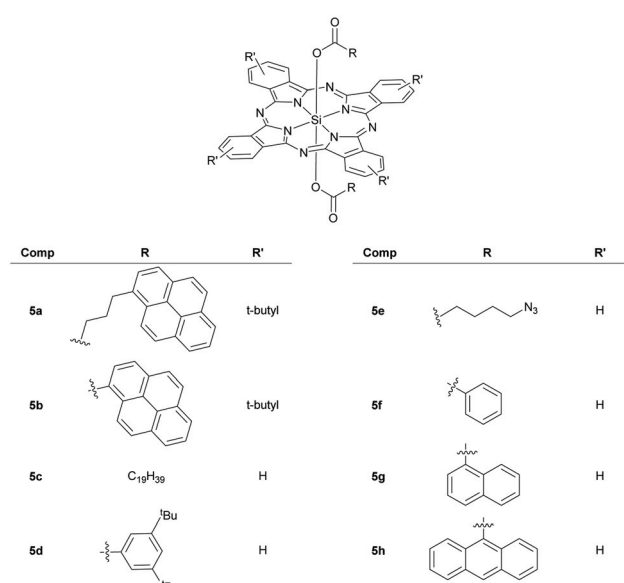


**Fig. 9** Chemical structures of bis-ester SiPc derivatives, **5a**–**5h**.

P3HT/PCBM solar cell devices.<sup>115</sup> The ternary devices with these variants displayed an increase of over 20% in  $J_{SC}$  and over 50% in PCE values compared to the baseline binary device. Among the variants, best fill factor and charge carrier mobility were obtained for the device constructed with **5a** (Fig. 9, Table 1).

In an attempt to further increase the light harvesting window up to 800 nm, SiNcs, having appropriate energy levels, were deployed alone or with SiPcs (Fig. 10).<sup>112,116</sup> The research group of Sellinger used a symmetrical 2,3-SiNc derivative, **26** with peripheral *t*-butyl groups and two axial trihexylsilylooxide groups as the only light harvesting additive in a ternary P3HT/

PMBC solar cell (Fig. 10A).<sup>116</sup> The presence of bulky *t*-butyl functional groups conferred higher solubility to **26** and the BHJ morphology of P3HT/PCBM was preserved even with excess dye incorporation. Thus, higher optimal dye loading contents up to 20% was achieved without causing a decrease in  $J_{SC}$ . The blending of **26** resulted in ~40% enhancement of  $J_{SC}$  values and a PCE of up to 4.9% was reported (Table 1).

In another example, Honda *et al.* blended a SiNc dye, **27** along with **4b**, as a fourth component in the polymer-fullerene-SiPc solar cell (Fig. 7, 10A, B and C).<sup>112</sup> The quaternary



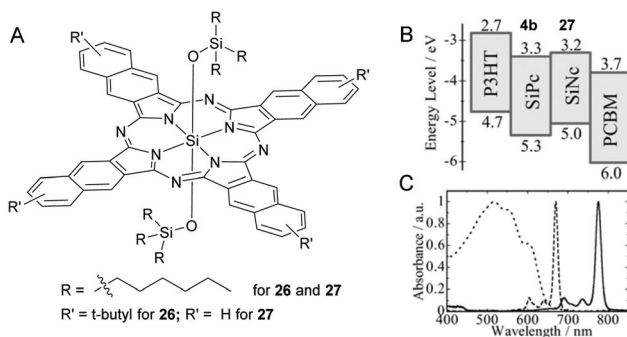


**Fig. 10** (A) Chemical structure of the SiPc dyes 26 and 27. (B) energy diagrams of P3HT, PCBM, SiPc 4b, and SiNc 27 (c) Absorption spectra of the P3HT/PCBM film (dotted line), SiPc 4b (broken line), and SiNc 27 (solid line) in solution. Adapted from ref. 112 with permissions from Royal Society of Chemistry.

solar cell P3HT/PCBM/SiPc(**4a**)/SiNc(**27**) exhibited a higher photoconversion efficiency (PCE) of 4.3% than the unblended (P3HT/PCBM) or ternary (P3HT/PCBM/SiPc(**4b**)) or (P3HT/PCBM/SiNc(**27**)) solar cells. The observed values for the quaternary device were  $J_{SC}$ ,  $V_{OC}$  and FF were  $10.9 \text{ mA cm}^{-2}$ , 0.57 V and 0.69 respectively at a loading content of 4.8 wt% for **4b** and 1.5 wt% for **27** (Table 1). This improvement in device performance was attributed to the efficient photocurrent generation in the broad absorption profile in the visible region stretching from 400 to 800 nm.

Ameri and co-workers fabricated a quaternary solar cell using SiNc, **28** and SiPc, **5b** containing axial pyrene units in order to investigate the effect of elongated  $\pi$ -systems on the device characteristics (Fig. 9 and 11A).<sup>117</sup> They observed an improved PCE of 3.89 at a loading content of 7.5 and 5 wt% respectively for **5b** and **28** as compared to the ternary blend solar cells with individual dyes (Table 1).

Instead of using two distinct SiPc and SiNc dyes, Sellinger *et al.* developed a hybrid SiNcPc, **29** bearing a mononaphtho triphthalocyanine core and investigated its photosensitizing properties in a DSSC (Fig. 11B).<sup>118</sup> A vinyl group was introduced in the mononaphthalocyanine ring to establish conjugation with an anchoring carboxylic acid unit. The hybrid dye, **29** exhibited high solubility, high extinction coefficients and desirable energy levels. The integration of **29** in solar devices resulted in high photocurrents of  $19.0 \text{ A cm}^{-2}$  and a total efficiency of 4.5% (Table 1).

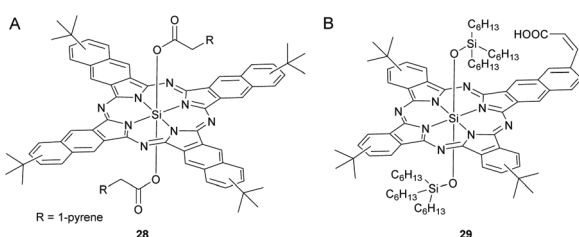


**Fig. 11** Chemical structures of dyes (A) **28** and (B) **29**. R denotes 1-pyrene group.

**3.2.2 SiPc as acceptors and donors in photovoltaic solar cells.** The promising traits of the SiPc dyes as additives prompted researchers to explore their donor and acceptor properties. Preliminary assessment of few SiPc variants (**4b**, **4c** and **4d**) as possible acceptors in binary blends P3HT/SiPc was carried out for the first time by Bender and co-workers (Fig. 7). The studies led to the conclusion that replacement of PCBM by SiPc results in  $\sim$ 50% increase in  $V_{OC}$  values, but a much lower PCE efficiencies of only  $\sim$ 1% when compared to the standard P3HT/PCBM donor acceptor pair (Table 1).<sup>40</sup>

In another report, the electron donating and accepting dual-nature functionalities of SiPcCl<sub>2</sub>, **1** and bis(pentafluorophenoxy)-SiPc, **3f** (Fig. 8) in un-optimized planar heterojunction (PHJ) solar cell devices were demonstrated (Fig. 8, Table 1).<sup>36</sup> Compound **3f** displayed superior donor and acceptor properties which improved the device performance as compared to **1**. These striking device characteristics of **3f** were partially attributed to the solid-state arrangement and improved  $\pi$ -shielding as evident from its X-ray crystal structure. On the contrary, such  $\pi$ - $\pi$  interactions were completely missing in the crystals of **1**. It was further noted that the frequency and position of the fluorine atoms in the axial phenoxy group governed the dual-characteristics of the SiPc derivatives.<sup>119</sup> The crude structure-activity analysis revealed SiPc analogues, **3g** and **3h** as potential donors and acceptors, respectively for future device configuration (Fig. 8, Table 1).

Samuel and co-workers investigated symmetrical SiPcs with axial bis-esters of eicosanoic acid (**5c**) and 3,5-di-*tert*-butylbenzoic acid (**5d**) as NIR absorbing dyes and electron acceptors in binary BHJ organic solar cells (Fig. 9, Table 1).<sup>120</sup> The best device characteristics were obtained on using PTB7, a dithiophene based polymer and **5d** as the donor acceptor pair at a 1 : 1.5 weight ratio and were attributed to the increased photocurrent and strong visible absorption of **5d**.

**3.2.3 SiPc as crosslinking agent in photovoltaic solar cells.** Lessard *et al.* reported a bis(6-azidohexanoate)SiPc dye, **5e** bearing crosslinking groups. The incorporation of this dye in a P3HT/PCBM BHJ solar cell led to dual functions as a ternary additive and an effective crosslinker (Fig. 9).<sup>121</sup> The baseline P3HT/PCBM binary device (without **5e**) suffered significant loss in  $J_{SC}$  and PCE values on exposure to a thermal ageing of 150 °C for 23 h owing to the phase separation and crystallization of the PCBM. Loading of the dye, **5e** in the device boosted the photocurrent generation in the near-*infra* red region implying a synergistic additive influence. Interestingly, the crosslinking ability of **5e** via the axial azides, preserved the BHJ morphology and retained the overall performance (PCE) by 97% after thermal ageing (Fig. 12).

#### 3.4 Applications of SiPc in OLEDs

SiPcs exhibit intense and narrow NIR luminescence spectra and thus find applications as emitters in organic light emitting diodes (OLEDs). Samuel and co-workers recently studied the optoelectronic properties and the electroluminescence of two SiPc derivatives, **5c** and **5d** (Fig. 9).<sup>120</sup> Both derivatives displayed electroluminescence features in OLEDs similar to their



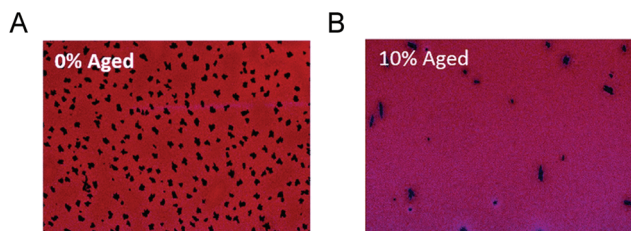


**Fig. 12** Microscopic images (20x magnification) of (A) after thermal ageing of baseline P3HT/PCBM devices with 0% **5e** (B) after thermal ageing of P3HT/PCBM devices with 10% **5e**. Adapted from ref. 121 with permission from The Royal Society of Chemistry.

photoluminescence profiles with a maxima around 698–709 nm and a narrow full width at half maxima (FWHM) of 21–27 nm. It was observed that doping of the emitting layer of the device with 10% **5c** resulted in better quality of OLEDs with fewer pinholes and reduced roughness as compared to **5d** indicating that structure of the axial ligands influence device characteristics (Fig. 13).

Instead of using long chain carbons to reduce aggregation and confer solubility, Greenham and co-workers chose carbon-efficient and electron withdrawing pentafluorophenoxy moieties as the axial ligands.<sup>122</sup> They deployed the SiPc derivative, **3f** as dopant red emitters in both solution-processed and vapour-deposited OLEDs (Fig. 8). Compound **3f** displayed a photoluminescence quantum yield value of 0.66 and a band gap of 1.77 eV. The OLED devices constructed with a polymeric host and **3f** as a guest showed narrow electroluminescence spectra (FWHM of 20 nm) with a maximum external quantum

efficiency (EQE) value of 2.5%. The vapour-deposited host : guest OLEDs incorporating 5 wt% doped **3f** displayed similar emission profile with maximum around 715 nm, albeit, with a much lower EQE value of ~0.09%. Though the energy transfer was clearly confirmed in this device, low EQE values indicated that a proper choice of host is crucial in order to achieve a significantly higher dopant emission over the host emission.

### 3.5 Applications of SiPc in OTFTs

Like other nitrogen heterocycle-based compounds,<sup>123,124</sup> certain SiPcs also possess electronic properties of n-type semiconductors.<sup>26</sup> Additionally, the readily tunable axial ligands, high field-effect mobility, robust environmental stability and ease of processability make them ideal to perform as organic thin film transistors (OTFTs).

Lessard *et al.*, first deployed SiPcs as n-type semiconductors in bottom-gate bottom-contact (BGBC) OTFT devices.<sup>125</sup> SiPc bis-esters with 1-benzoic (**5f**), 1-naphthoic (**5g**) and 9-anthroic (**5h**) acid axial pendants were explored to establish a link between solid state arrangements of the semiconductors and the overall device performances (Fig. 9). The varying degree of  $\pi$ -bonding interactions of the Pc chromophores was expected to partly affect the 2D charge transfer pathways in the devices. The crystal structures revealed that **5f** and **5g** showed significant parallel stacking of the Pc rings. This probably led to higher electron field effect mobility ( $\mu_e$ ) and increased on-current ( $I_{on}$ ) in devices with **5f** and **5g**. Although **5g** revealed the closest  $\pi$ - $\pi$  interactions, its device performance was lower than that of **5f**. On the other hand, the bulky anthracene group hindered the overlap of the Pc rings and devices with **5h** displayed lowest  $\mu_e$  and  $I_{on}$  values. However, devices with **5h** exhibited the lowest threshold voltage ( $V_T$ ). This is possibly because the lowest unoccupied molecular orbital (LUMO) of **5h** was energetically comparable to the work function of gold. Overall, **5f** outclassed the other SiPcs in the series in terms of device performance. Further increment of device performance of **5f** was achieved with octyltrichlorosilane (OTS) dielectric modification and a substrate temperature of 200 °C maintained during deposition.

Motivated by these results, Lessard *et al.*, investigated the behaviour of fluorophenoxy derivatives of SiPc as n-type transistors.<sup>126,127</sup> It was noticed that the frequency and position of fluorine atoms affected electron mobility and the compounds **3f**–**3h** exhibited some ambipolarity of charge transport (Fig. 8). In the series, devices built with **3f** deposited on OTS-modified surface displayed superior performance. Taken together, these reports demonstrated the potential roles of axial substituents in governing the device performances and hinted towards a possibility of obtaining high performance SiPc based n-type semiconductors.

### 3.6 Applications in photocatalysis

The design of tetrapyrrole complexes and investigation of their photocatalytic behaviour stemmed from the key roles played by naturally occurring tetrapyrrole complexes (e.g. chlorophyll) in photosynthesis.<sup>128,129</sup> In this context, SiPcs are recently

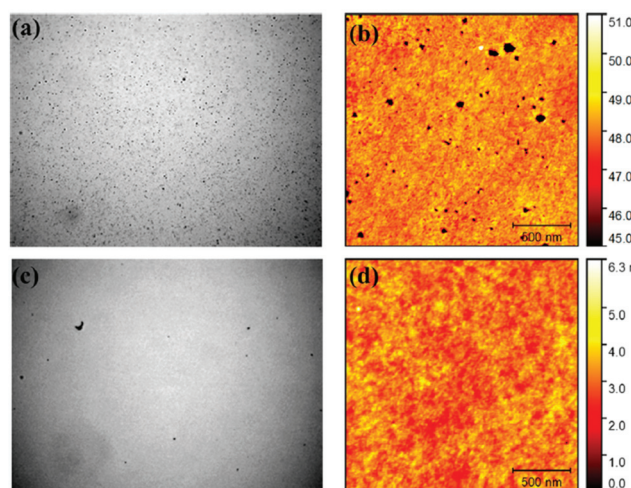


**Fig. 13** Optical microscopy [(a and c); 150  $\times$  113  $\mu\text{m}^2$  each] and atomic-force microscopy [(b and d); 2  $\times$  2  $\mu\text{m}^2$  each; 500 nm scale bar] of films ITO/PEDOT:PSS/PVK/CBP:PBD:SiPc (30 : 60 : 10; SiPc = **5c** or **5d**; 30 nm). The film doped with **5d** [(a and b)] has more pinholes and higher RMS roughness  $R_a$  = 0.72 nm than the film doped with **5c** [(c and d);  $R_a$  = 0.4 nm]. Adapted with permission from ref. 120. Further permissions related to the material excerpted should be directed to the ACS (<https://pubs.acs.org/doi/10.1021/acsami.5b12408>).



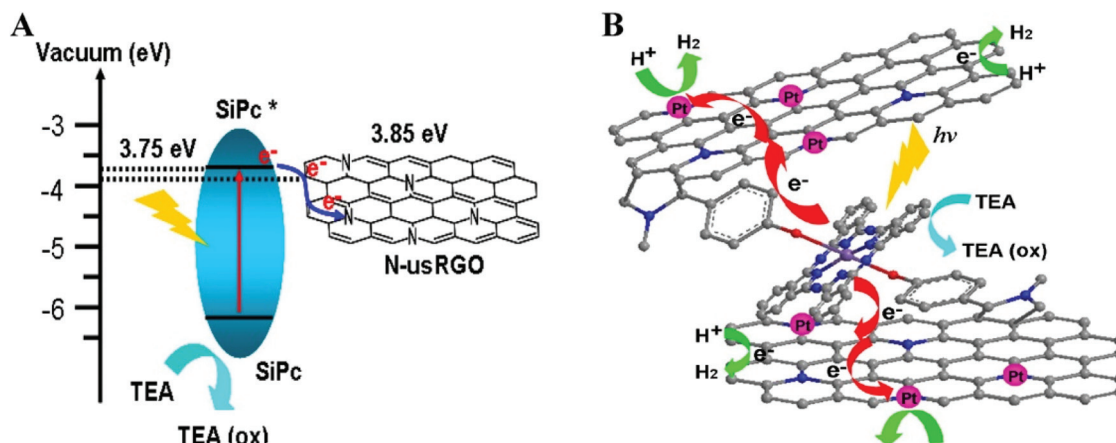


Fig. 14 (A) Energy band structure diagram of heterostructure between N-usRGO and SiPc and (B) Electron transfer processes and evolution of hydrogen in N-usRGO/SiPc/Pt photocatalyst. Reprinted with permission from ref. 133. Copyright (2015) American Chemical Society.

being explored for potential applications in solar energy conversion and homogeneous photocatalysis. The fulfilling criteria of SiPcs to function as photocatalysts include: (i) robust photostability, (ii) intense absorption features in the solar spectrum which are tunable at the molecular level and (iii) ability to initiate photoinduced electron transfer reactions.<sup>130</sup>

Knör and co-workers synthesized a cationic, water soluble SiPc, **3i** and investigated its potential for construction of hydrogen evolving photocatalytic systems (Fig. 8, see above).<sup>131</sup> Compound **3i** reacted with aerial oxygen predominantly through a type II sensitization mechanism involving formation of singlet oxygen. Trace amounts of 1,4-benzoquinone and triethanolamine efficiently quenched the fluorescence signal of **3i** following a Stern–Volmer kinetics of bimolecular quenching mechanism. Excess of triethanolamine led to rapid accumulation of permanent photoredox products of **3i**. This confirmed the presence of a photoinduced electron transfer process possibly involving reduced Pc  $\pi$ -radical anion intermediates. Such radical species play important roles in mediating photochemical water splitting, thereby making SiPcs attractive candidates for construction of solar energy driven catalytic systems.

In another study, the catalytic behaviour of another SiPc derivative, **3j**, was investigated using the 4-nitrophenol degradation probe reaction (Fig. 8, see above).<sup>132</sup> Visible light induced degradation of 4-nitrophenol was observed with catalytic amounts of **3j** and hydrogen peroxide as a source of oxygen. Hydroquinone and benzoquinone were determined as the major and minor photoproducts respectively. A substrate/oxidant/catalyst ratio of 2000/500/1 resulted in 88% conversion with a turnover number of 1758 and turnover frequency of 586 for **3j**. Interestingly, photoconversion (37%) of 4-nitrophenol was observed without hydrogen peroxide, indicating the ability of **3j** to act as a photocatalyst in absence of any oxygen source.

Recent reports exploited covalently functionalized SiPc-graphene based organic hybrid composites as improved solar catalysts.<sup>133,134</sup> SiPc covalently functionalized with N-doped ultrasmall reduced graphene oxide (N-usRGO/SiPc) displayed

strong absorption in the visible spectrum.<sup>133</sup> The fluorescence quenching (90%) of SiPc and improved photocurrent responses for N-usRGO/SiPc demonstrated the efficient photo-induced electron transfer process from SiPc to N-usRGO through covalent bonds (Fig. 14A). These properties attributed to higher visible light induced catalytic activity of (N-usRGO/SiPc) in comparison to SiPc free N-usRGO. Platinum nanoparticles (Pt NP, 5 wt% Pt) deposited on N-heteroatoms of graphene acted as cocatalyst and further enhanced the catalytic performance of the composite (Fig. 14B). Pt NP decorated N-usRGO/SiPc construct produced a maximum of  $4.5 \mu\text{mol mg}^{-1}$  of hydrogen from water on 6 h of UV-vis irradiation. The proposed mechanism suggests sequential shuttling of electrons from light harvesting SiPc to graphene layers and consequently to Pt NP where water molecules accept electrons and evolve hydrogen (Fig. 14B). Finally, triethanolamine (TEA) donates electron to excited SiPc and brings it back to the ground state (Fig. 14B).

Lu *et al.* observed that addition of surfactants like cetyltrimethylammonium bromide (CTAB) prevented aggregation and boosted the photocatalytic behaviour of a SiPc(phenyl) covalently functionalized and Pt NP loaded graphene construct, SiPc(phenyl)<sub>2</sub>G<sub>2</sub>/Pt (Ref: IntJHydE2016).<sup>134</sup> The integrated photocatalytic system, SiPc(phenyl)<sub>2</sub>G<sub>2</sub>/Pt/CTAB produced  $18.2 \mu\text{mol mg}^{-1}$  of hydrogen on 10 h or UV-visible irradiation. These studies together established the potential of SiPcs in construction of water splitting photocatalytic systems.

## 4. Conclusions and perspectives

Despite their long existence, SiPcs continue to attract unabated attention due to their emerging properties and applications. Like most other phthalocyanines, SiPcs have gained profound recognition as far-red and NIR photodynamic therapeutic and fluorescence imaging agents. Recent findings corroborated the photodissociative nature of the axial ligands and added a new

dimension to these old molecules. Novel mechanisms proposed to be involved in photouncaging and photoimmuno-therapy have recommenced exploration of SiPcs in light-based therapeutic approaches, other than PDT. While the Si–O bonds exhibit additive and/or oxygen dependent photocleavage, the Si–C bonds can rapidly dissociate without any dependence on oxygen or redox reagents. Besides medicinal applications, SiPcs are rapidly acquiring a foothold in the emerging fields of photovoltaics, organic electronics and photocatalysis. However, thoughtful considerations of energy levels, bulk heterojunction morphology, solubility and crystallinity are essential while designing SiPc variants in order to observe enhanced efficiency and performances of the devices. Though few SiPc molecules seem propitious, further structure–activity studies are required to correlate the structural modifications with the device characteristics. Altogether, the promising results bode well for future explorations of SiPc in multifaceted research areas.

However, these outstanding applications rest heavily on the structural modifications of the axial and phthalocyanine ring positions of SiPcs. The synthetic challenges to construct SiPc variants have been the bottleneck of this field and have impeded many applications. Oftentimes, the syntheses of SiPcs employ harsh reagents and drastic conditions. Furthermore, the reactions suffer from low synthetic yields and produce multiple undesired products. The purification techniques are complicated and laborious. Thus, the current scenario highlights the need for convenient and reliable synthetic methodology using non-hazardous and affordable reagents. Future efforts to define elegant synthetic approaches will be of paramount importance for complete realization of potential of SiPcs in phototherapy and energy harvesting applications.

## Conflicts of interest

M. C. T. H. is a founder and shareholder of Light Switch Bio, LLC., a startup company that is developing light-based therapeutics for commercial applications.

## Acknowledgements

This work was supported by the Virginia Commonwealth Health Research Board (236-03-16).

## Notes and references

- 1 P. A. Barrett, C. E. Dent and R. P. Linstead, Phthalocyanines. Part VII. Phthalocyanine as a co-ordinating group. A general investigation of the metallic derivatives, *J. Chem. Soc.*, 1936, **382**, 1719–1736.
- 2 J. A. Elvidge and R. P. Linstead, Conjugated macrocycles. Part XXVII. The formation of tetrazaporphins from imi-

dines. Tribenzotetrazaporphin, *J. Chem. Soc.*, 1955, 3536–3544.

- 3 R. P. Linstead and A. R. Lowe, Phthalocyanines. Part III. Preliminary experiments on the preparation of phthalocyanines from phthalonitrile, *J. Chem. Soc.*, 1934, **214**, 1022–1027.
- 4 J. M. Robertson, An X-ray study of the structure of the phthalocyanines. Part I. The metal-free, nickel, copper, and platinum compounds, *J. Chem. Soc.*, 1935, **136**, 615–621.
- 5 H. Lu and N. Kobayashi, Optically Active Porphyrin and Phthalocyanine Systems, *Chem. Rev.*, 2016, **116**, 6184–6261.
- 6 B. L. Wheeler, G. Nagasubramanian, A. J. Bard, L. A. Schechtman and M. E. Kenney, A silicon phthalocyanine and a silicon naphthalocyanine: synthesis, electrochemistry, and electrogenerated chemiluminescence, *J. Am. Chem. Soc.*, 1984, **106**, 7404–7410.
- 7 M. Matsuoka, Phthalocyanine and Naphthalocyanine Dyes, in *Infrared Absorbing Dyes. Topics in Applied Chemistry*, ed. M. Matsuoka, Springer, Boston, MA, 1990, pp. 45–55.
- 8 S. Kakade, R. Ghosh and D. K. Palit, Excited State Dynamics of Zinc–Phthalocyanine Nanoaggregates in Strong Hydrogen Bonding Solvents, *J. Phys. Chem. C*, 2012, **116**, 15155–15166.
- 9 G. v. Bünau and J. B. Birks, Photophysics of Aromatic Molecules. Wiley-Interscience, London 1970. 704 Seiten. Preis: 210s, *Ber. Bunsenges. Phys. Chem.*, 1970, **74**, 1294–1295.
- 10 J. M. Dąbrowski, B. Pucelik, A. Regiel-Futyra, M. Brindell, O. Mazuryk, A. Kyzioł, G. Stochel, W. Macyk and L. G. Arnaut, Engineering of relevant photodynamic processes through structural modifications of metallotetrapyrrolic photosensitizers, *Coord. Chem. Rev.*, 2016, **325**, 67–101.
- 11 X. Li, B.-D. Zheng, X.-H. Peng, S.-Z. Li, J.-W. Ying, Y. Zhao, J.-D. Huang and J. Yoon, Phthalocyanines as medicinal photosensitizers: Developments in the last five years, *Coord. Chem. Rev.*, 2019, **379**, 147–160.
- 12 C. G. Claessens, U. Hahn and T. Torres, Phthalocyanines: From outstanding electronic properties to emerging applications, *Chem. Rec.*, 2008, **8**, 75–97.
- 13 R. D. Joyner and M. E. Kenney, Phthalocyaninosilicon Compounds, *Inorg. Chem.*, 1962, **1**, 236–238.
- 14 J.-W. Hofman, F. van Zeeland, S. Turker, H. Talsma, S. A. G. Lambrechts, D. V. Sakharov, W. E. Hennink and C. F. van Nostrum, Peripheral and Axial Substitution of Phthalocyanines with Solketal Groups: Synthesis and In Vitro Evaluation for Photodynamic Therapy, *J. Med. Chem.*, 2007, **50**, 1485–1494.
- 15 H. Li, T. J. Jensen, F. R. Fronczek and M. G. H. Vicente, Syntheses and Properties of a Series of Cationic Water-Soluble Phthalocyanines, *J. Med. Chem.*, 2008, **51**, 502–511.
- 16 J. C. Berlin, *Silicon phthalocyanines for photodynamic therapy*, Phd Thesis, Case Western Reserve University, 2006.



17 E. van de Winckel, B. David, M. M. Simoni, J. A. González-Delgado, A. de la Escosura, Â. Cunha and T. Torres, Octacationic and axially di-substituted silicon(IV) phthalocyanines for photodynamic inactivation of bacteria, *Dyes Pigm.*, 2017, **145**, 239–245.

18 K. Sato, K. Ando, S. Okuyama, S. Moriguchi, T. Ogura, S. Totoki, H. Hanaoka, T. Nagaya, R. Kokawa, H. Takakura, M. Nishimura, Y. Hasegawa, P. L. Choyke, M. Ogawa and H. Kobayashi, Photoinduced Ligand Release from a Silicon Phthalocyanine Dye Conjugated with Monoclonal Antibodies: A Mechanism of Cancer Cell Cytotoxicity after Near-Infrared Photoimmunotherapy, *ACS Cent. Sci.*, 2018, **4**, 1559–1569.

19 E. D. Anderson, A. P. Gorka and M. J. Schnermann, Near-infrared uncaging or photosensitizing dictated by oxygen tension, *Nat. Commun.*, 2016, **7**, 13378.

20 M. D. Maree, N. Kuznetsova and T. Nyokong, Silicon octaphenoxyphthalocyanines: photostability and singlet oxygen quantum yields, *J. Photochem. Photobiol. A*, 2001, **140**, 117–125.

21 Y. Cheng, T. L. Doane, C.-H. Chuang, A. Ziady and C. Burda, Near infrared light-triggered drug generation and release from gold nanoparticle carriers for photodynamic therapy, *Small*, 2014, **10**, 1799–1804.

22 J. Li, Y. Yang, P. Zhang, J. R. Sounik and M. E. Kenney, Synthesis, properties and drug potential of the photosensitive alkyl- and alkylsiloxy-ligated silicon phthalocyanine Pc 227, *Photochem. Photobiol. Sci.*, 2014, **13**, 1690–1698.

23 P.-C. Lo, M. S. Rodriguez-Morgade, R. K. Pandey, D. K. P. Ng, T. Torres and F. Dumoulin, The unique features and promises of phthalocyanines as advanced photosensitisers for photodynamic therapy of cancer, *Chem. Soc. Rev.*, 2020, **49**, 1041–1056.

24 R. D. Joyner, J. Cekada, R. G. Linck and M. E. Kenney, Diphenoxysilicon phthalocyanine, *J. Inorg. Nucl. Chem.*, 1960, **15**, 387–388.

25 M. K. Lowery, A. J. Starshak, J. N. Esposito, P. C. Krueger and M. E. Kenney, Dichloro(phthalocyanino)silicon, *Inorg. Chem.*, 1965, **4**, 128.

26 N. J. Yutronkie, T. M. Grant, O. A. Melville, B. H. Lessard and J. L. Brusso, Old Molecule, New Chemistry: Exploring Silicon Phthalocyanines as Emerging N-Type Materials in Organic Electronics, *Materials*, 2019, **12**, 1334.

27 R. Rafaeloff, F. J. Kohl, P. C. Krueger and M. E. Kenney, New group IV phthalocyanines, *J. Inorg. Nucl. Chem.*, 1966, **28**, 899–902.

28 J. N. Esposito, J. E. Lloyd and M. E. Kenney, The Synthesis and Physical Properties of Some Organo- and Organosiloxysilicon Phthalocyanines, *Inorg. Chem.*, 1966, **5**, 1979–1984.

29 T. M. Grant, V. McIntyre, J. Vestfrid, H. Raboui, R. T. White, Z.-H. Lu, B. H. Lessard and T. P. Bender, Straightforward and Relatively Safe Process for the Fluoride Exchange of Trivalent and Tetravalent Group 13 and 14 Phthalocyanines, *ACS Omega*, 2019, **4**, 5317–5326.

30 B. H. Lessard, J. D. Dang, T. M. Grant, D. Gao, D. S. Seferos and T. P. Bender, Bis(tri-n-hexylsilyl oxide) Silicon Phthalocyanine: A Unique Additive in Ternary Bulk Heterojunction Organic Photovoltaic Devices, *ACS Appl. Mater. Interfaces*, 2014, **6**, 15040–15051.

31 J.-D. Huang, S. Wang, P.-C. Lo, W.-P. Fong, W.-H. Ko and D. K. P. Ng, Halogenated silicon(IV) phthalocyanines with axial poly(ethylene glycol) chains. Synthesis, spectroscopic properties, complexation with bovine serum albumin and in vitro photodynamic activities, *New J. Chem.*, 2004, **28**, 348–354.

32 J. Mao, Y. Zhang, J. Zhu, C. Zhang and Z. Guo, Molecular combo of photodynamic therapeutic agent silicon(IV) phthalocyanine and anticancer drug cisplatin, *Chem. Commun.*, 2009, 908–910.

33 D. Demirkapı, A. Şirin, B. Turanlı-Yıldız, Z. P. Çakar and B. Ş. Sesalan, The synthesis of new silicon phthalocyanines and analysis of their photochemical and biological properties, *Synth. Met.*, 2014, **187**, 152–159.

34 L. Luan, L. Ding, J. Shi, W. Fang, Y. Ni and W. Liu, Effect of Axial Ligands on the Molecular Configurations, Stability, Reactivity, and Photodynamic Activities of Silicon Phthalocyanines, *Chem. – Asian J.*, 2014, **9**, 3491–3497.

35 W. Harada, M. Hirahara, T. Togashi, M. Ishizaki, M. Kurihara, M. Haga and K. Kanaizuka, Wisely Designed Phthalocyanine Derivative for Convenient Molecular Fabrication on a Substrate, *Langmuir*, 2018, **34**, 1321–1326.

36 B. H. Lessard, R. T. White, M. AL-Amar, T. Plint, J. S. Castrucci, D. S. Josey, Z.-H. Lu and T. P. Bender, Assessing the Potential Roles of Silicon and Germanium Phthalocyanines in Planar Heterojunction Organic Photovoltaic Devices and How Pentafluoro Phenoxylation Can Enhance  $\pi$ – $\pi$  Interactions and Device Performance, *ACS Appl. Mater. Interfaces*, 2015, **7**, 5076–5088.

37 X. Leng, C.-F. Choi, P.-C. Lo and D. K. P. Ng, Assembling a Mixed Phthalocyanine–Porphyrin Array in Aqueous Media through Host–Guest Interactions, *Org. Lett.*, 2007, **9**, 231–234.

38 J. T. F. Lau, P.-C. Lo, W.-P. Fong and D. K. P. Ng, Preparation and Photodynamic Activities of Silicon(IV) Phthalocyanines Substituted with Permethylated  $\beta$ -Cyclodextrins, *Chem. – Eur. J.*, 2011, **17**, 7569–7577.

39 H. M. Anula, J. C. Berlin, H. Wu, Y.-S. Li, X. Peng, M. E. Kenney and M. A. J. Rodgers, Synthesis and Photophysical Properties of Silicon Phthalocyanines with Axial Siloxy Ligands Bearing Alkylamine Termini, *J. Phys. Chem. A*, 2006, **110**, 5215–5223.

40 M.-T. Dang, T. M. Grant, H. Yan, D. S. Seferos, B. H. Lessard and T. P. Bender, Bis(tri-n-alkylsilyl oxide) silicon phthalocyanines: a start to establishing a structure property relationship as both ternary additives and non-fullerene electron acceptors in bulk heterojunction organic photovoltaic devices, *J. Mater. Chem. A*, 2017, **5**, 12168–12182.



41 T. Gessner, R. Sens, W. Ahlers and C. Vamvakaris, Preparation of silicon phthalocyanines and germanium phthalocyanines and related substances, *U.S. Patent*, US20100113767A1, 2010.

42 Y.-S. Li, S. I. A. Zaidi, M. A. J. Rodgers, H. Mukhtar, M. E. Kenney, N. L. Oleinick, J. He, H. E. Larkin and B. D. Rihter, The Synthesis, Photophysical and Photobiological Properties and in vitro Structure-Activity Relationships of a Set of Silicon Phthalocyanine PDT Photosensitizers, *Photochem. Photobiol.*, 1997, **65**, 581–586.

43 X. Peng, D. R. Draney and J. Chen, Phthalocyanine Dyes, *U.S. Patent*, US7005518B2, 2004.

44 M. C. Vebber, T. M. Grant, J. L. Brusso and B. H. Lessard, Bis(trialkylsilyl oxide) Silicon Phthalocyanines: Understanding the Role of Solubility in Device Performance as Ternary Additives in Organic Photovoltaics, *Langmuir*, 2020, **36**, 2612–2621.

45 A. K. Sinha and B. K. Mandal, Thin Polyurethane Films of Polyhydroxysilicon Phthalocyanine and Bis-phthalocyanine Derivatives, *Polym. J.*, 1995, **27**, 1079–1084.

46 D. W. DeWulf, J. K. Leland, B. L. Wheeler, A. J. Bard, D. A. Batzel, D. R. Dininny and M. Kenney, Isolation, spectroscopic properties, and electrochemical properties of two oligomeric silicon phthalocyanines, *Inorg. Chem.*, 1987, **26**, 266–270.

47 Y. Yang, B. Samas, V. O. Kennedy, D. Macikenas, B. L. Chaloux, J. A. Miller, R. L. Speer, J. Protasiewicz, A. A. Pinkerton and M. E. Kenney, Long, Directional Interactions in Cofacial Silicon Phthalocyanine Oligomers, *J. Phys. Chem. A*, 2011, **115**, 12474–12485.

48 K. Oniwa, S. Shimizu, Y. Shiina, T. Fukuda and N. Kobayashi, A  $\mu$ -oxo hetero dimer of silicon phthalocyanine and naphthalocyanine, *Chem. Commun.*, 2013, **49**, 8341–8343.

49 Z. Li and M. Lieberman, Axial Reactivity of Soluble Silicon (IV) Phthalocyanines, *Inorg. Chem.*, 2001, **40**, 932–939.

50 J. B. Davison and K. J. Wynne, Silicon Phthalocyanine-Siloxane Polymers: Synthesis and  $^1\text{H}$  Nuclear Magnetic Resonance Study, *Macromolecules*, 1978, **11**, 186–191.

51 C. A. Barker, K. S. Findlay, S. Bettington, A. S. Batsanov, I. F. Perepichka, M. R. Bryce and A. Beeby, Synthesis of new axially-disubstituted silicon-phthalocyanine derivatives: optical and structural characterisation, *Tetrahedron*, 2006, **62**, 9433–9439.

52 K. Mitra, M. Samsó, C. E. Lyons and M. C. T. Hartman, Hyaluronic acid grafted nanoparticles of a platinum(II)-silicon(IV) phthalocyanine conjugate for tumor and mitochondria-targeted photodynamic therapy in red light, *J. Mater. Chem. B*, 2018, **6**, 7373–7377.

53 A. K. Pal, S. Varghese, D. B. Cordes, A. M. Z. Slawin, I. D. W. Samuel and E. Zysman-Colman, Near-Infrared Fluorescence of Silicon Phthalocyanine Carboxylate Esters, *Sci. Rep.*, 2017, **7**, 12282.

54 C. Farren, S. FitzGerald, M. R. Bryce, A. Beeby and A. S. Batsanov, Synthesis, structure and optical characterisation of silicon phthalocyanine bis-esters, *J. Chem. Soc., Perkin Trans. 2*, 2002, 59–66.

55 C. Farren, C. A. Christensen, S. FitzGerald, M. R. Bryce and A. Beeby, Synthesis of Novel Phthalocyanine-Tetrathiafulvalene Hybrids; Intramolecular Fluorescence Quenching Related to Molecular Geometry, *J. Org. Chem.*, 2002, **67**, 9130–9139.

56 W. Rodríguez-Córdoba, R. Noria, C. A. Guarín and J. Peón, Ultrafast Photosensitization of Phthalocyanines through Their Axial Ligands, *J. Am. Chem. Soc.*, 2011, **133**, 4698–4701.

57 Y.-S. Li and M. E. Kenney, Methods of syntheses of phthalocyanine compounds, *U.S. Patent*, US5763602A, 1998.

58 N. L. Oleinick, A. R. Antunez, M. E. Clay, B. D. Rihter and M. E. Kenney, New phthalocyanine photosensitizers for photodynamic therapy, *Photochem. Photobiol.*, 1993, **57**, 242–247.

59 P.-C. Lo, J.-D. Huang, D. Y. Y. Cheng, E. Y. M. Chan, W.-P. Fong, W.-H. Ko and D. K. P. Ng, New Amphiphilic Silicon(IV) Phthalocyanines as Efficient Photosensitizers for Photodynamic Therapy: Synthesis, Photophysical Properties, and in vitro Photodynamic Activities, *Chem. – Eur. J.*, 2004, **10**, 4831–4838.

60 B.-Y. Zheng, L. Wang, Q.-Y. Hu, J. Shi, M.-R. Ke and J.-D. Huang, Novel unsymmetrical silicon(IV) phthalocyanines as highly potent anticancer photosensitizers. Synthesis, characterization, and in vitro photodynamic activities, *Dyes Pigm.*, 2020, **177**, 108286.

61 J. T. F. Lau, P.-C. Lo, Y.-M. Tsang, W.-P. Fong and D. K. P. Ng, Unsymmetrical  $\beta$ -cyclodextrin-conjugated silicon(IV) phthalocyanines as highly potent photosensitizers for photodynamic therapy, *Chem. Commun.*, 2011, **47**, 9657–9659.

62 Q. Liu, M. Pang, S. Tan, J. Wang, Q. Chen, K. Wang, W. Wu and Z. Hong, Potent peptide-conjugated silicon phthalocyanines for tumor photodynamic therapy, *J. Cancer*, 2018, **9**, 310–320.

63 Z. Li and M. Lieberman, Synthesis and characterization of functionalized silicon phthalocyanines for fabrication of self-assembled monolayers, *Supramol. Sci.*, 1998, **5**, 485–489.

64 M. Hanack, K. Mitulla, G. Pawlowski and L. R. Subramanian, Synthesis and properties of a new kind of one-dimensional conductor VIII. Synthesis and characterization of trans-bis-1-alkynyl substituted silicon, germanium, tin phthalocyanines and germanium hemiporphrazines, *J. Organomet. Chem.*, 1981, **204**, 315–325.

65 K. Tamao, M. Akita, H. Kato and M. Kumada, Electrophilic cleavage reactions of carbon-silicon bonds in neutral hexacoordinate silicon compounds: diorgano (phthalocyaninato)silicon, *J. Organomet. Chem.*, 1988, **341**, 165–179.

66 J. Li, *Silicon phthalocyanines for photodynamic therapy of studies*, PhD Thesis, Case Western Reserve University, 2008.



67 A. G. Gürek, G. Appel, R. P. Mikalo and D. Schmeißer, Synthesis of dihydroxy silicon phthalocyanine tetrasulfonic acid and poly- $\mu$ -oxo silicon phthalocyanine tetrasulfonic acid, *J. Porphyrins Phthalocyanines*, 2001, **5**, 751–757.

68 D. Woehrle, M. Eskes, K. Shigehara and A. Yamada, A Simple Synthesis of 4,5-Disubstituted 1,2-Dicyanobenzenes and 2,3,9,10,16,17,23,24-Octasubstituted Phthalocyanines, *Synthesis*, 1993, **1993**, 194–196.

69 T. Furuyama, T. Ishii, N. Ieda, H. Maeda, M. Segi, M. Uchiyama and H. Nakagawa, Cationic axial ligands on sulfur substituted silicon(iv) phthalocyanines: improved hydrophilicity and exceptionally red-shifted absorption into the NIR region, *Chem. Commun.*, 2019, **55**, 7311–7314.

70 G. Cheng, G. Hao, H. Wu, Y.-S. Li and M. E. Kenney, Methods for inserting silicon into phthalocyanines and naphthalocyanines, *U.S. Patent*, US5872248A, 1999.

71 S. Foley, G. Jones, R. Liuzzi, D. J. McGarvey, M. H. Perry and T. G. Truscott, The synthesis and photophysical properties of polyether substituted phthalocyanines of potential use in photodynamic therapy, *J. Chem. Soc., Perkin Trans. 2*, 1997, **2**, 1725–1730.

72 S. I. Büyükekş, S. Z. Topal and D. Atilla, Novel Silicon Phthalocyanines Bearing Triethylene Glycol Groups: Photophysical and Photochemical Properties as well as pH-Induced Spectral Behaviour, *J. Fluoresc.*, 2017, **27**, 1257–1266.

73 J. J. Bergkamp, B. D. Sherman, E. Mariño-Ochoa, R. E. Palacios, G. Cosa, T. A. Moore, D. Gust and A. L. Moore, Synthesis and characterization of silicon phthalocyanines bearing axial phenoxy groups for attachment to semiconducting metal oxides, *J. Porphyrins Phthalocyanines*, 2011, **15**, 943–950.

74 P.-C. Lo, C. M. H. Chan, J.-Y. Liu, W.-P. Fong and D. K. P. Ng, Highly Photocytotoxic Glucosylated Silicon(iv) Phthalocyanines. Effects of Peripheral Chloro Substitution on the Photophysical and Photodynamic Properties, *J. Med. Chem.*, 2007, **50**, 2100–2107.

75 R. F. Devlin, W. B. Dandliker and P. O. G. Arrhenius, Fluorescence immunoassays using fluorescence dyes free of aggregation and serum binding, *U.S. Patent*, US6060598A, 2000.

76 M. Lam, M. L. Dimaano, P. Oyetakin-White, M. A. Retuerto, J. Chandra, P. K. Mukherjee, M. A. Ghannoum, K. D. Cooper and E. D. Baron, Silicon phthalocyanine 4 phototoxicity in *Trichophyton rubrum*, *Antimicrob. Agents Chemother.*, 2014, **58**, 3029–3034.

77 A. Galstyan, R. Schiller and U. Dobrindt, Boronic Acid Functionalized Photosensitizers: A Strategy To Target the Surface of Bacteria and Implement Active Agents in Polymer Coatings, *Angew. Chem., Int. Ed.*, 2017, **56**, 10362–10366.

78 B. Aru, A. Günay, E. Şenkuytu, G. Yanikkaya Demirel, A. G. Gürek and D. Atilla, A Translational Study of a Silicon Phthalocyanine Substituted with a Histone Deacetylase Inhibitor for Photodynamic Therapy, *ACS Omega*, 2020, **5**, 25854–25867.

79 K. Li, W. Dong, Q. Liu, G. Lv, M. Xie, X. Sun, L. Qiu and J. Lin, A biotin receptor-targeted silicon(iv) phthalocyanine for in vivo tumor imaging and photodynamic therapy, *J. Photochem. Photobiol. B*, 2019, **190**, 1–7.

80 M. Mitsunaga, M. Ogawa, N. Kosaka, L. T. Rosenblum, P. L. Choyke and H. Kobayashi, Cancer cell-selective in vivo near infrared photoimmunotherapy targeting specific membrane molecules, *Nat. Med.*, 2011, **17**, 1685–1691.

81 J. T. F. Lau, P.-C. Lo, X.-J. Jiang, Q. Wang and D. K. P. Ng, A Dual Activatable Photosensitizer toward Targeted Photodynamic Therapy, *J. Med. Chem.*, 2014, **57**, 4088–4097.

82 R. Devlin, R. M. Studholme, W. B. Dandliker, E. Fahy, K. Blumeyer and S. S. Ghosh, Homogeneous detection of nucleic acids by transient-state polarized fluorescence, *Clin. Chem.*, 1993, **39**, 1939–1943.

83 G. T. Walker, J. G. Nadeau, C. P. Linn, R. F. Devlin and W. B. Dandliker, Strand displacement amplification (SDA) and transient-state fluorescence polarization detection of *Mycobacterium tuberculosis* DNA, *Clin. Chem.*, 1996, **42**, 9–13.

84 X. Peng, D. R. Draney, W. M. Volcheck, G. R. Bashford, D. T. Lamb, D. L. Grone, Y. Zhang and C. M. Johnson, Phthalocyanine dye as an extremely photostable and highly fluorescent near-infrared labeling reagent, *Proc. SPIE-Int. Soc. Opt. Eng.*, 2006, **6097**, 60970E.

85 N. Masilela and T. Nyokong, The synthesis and photophysical properties of novel cationic tetra pyridilox substituted aluminium, silicon and titanium phthalocyanines in water, *J. Lumin.*, 2010, **130**, 1787–1793.

86 M. Göksel, Z. Biyiklioglu and M. Durmuş, The water soluble axially disubstituted silicon phthalocyanines: photophysical properties and in vitro studies, *JBIC*, 2017, **22**, 953–967.

87 X. Li, J. F. Lovell, J. Yoon and X. Chen, Clinical development and potential of photothermal and photodynamic therapies for cancer, *Nat. Rev. Clin. Oncol.*, 2020, **17**, 657–674.

88 P. Agostinis, K. Berg, K. A. Cengel, T. H. Foster, A. W. Girotti, S. O. Gollnick, S. M. Hahn, M. R. Hamblin, A. Juzeniene, D. Kessel, M. Korbelik, J. Moan, P. Mroz, D. Nowis, J. Piette, B. C. Wilson and J. Golab, Photodynamic therapy of cancer: an update, *Ca-Cancer J. Clin.*, 2011, **61**, 250–281.

89 E. D. Baron, C. L. Malbasa, D. Santo-Domingo, P. Fu, J. D. Miller, K. K. Hanneman, A. H. Hsia, N. L. Oleinick, V. C. Colussi and K. D. Cooper, Silicon phthalocyanine (pc 4) photodynamic therapy is a safe modality for cutaneous neoplasms: results of a phase 1 clinical trial, *Lasers Surg. Med.*, 2010, **42**, 888–895.

90 M. A. Hutmick, S. Ahsanuddin, L. Guan, M. Lam, E. D. Baron and J. K. Pokorski, PEGylated Dendrimers as Drug Delivery Vehicles for the Photosensitizer Silicon Phthalocyanine Pc 4 for Candidal Infections, *Biomacromolecules*, 2017, **18**, 379–385.



91 Y. Cheng, J. D. Meyers, A.-M. Broome, M. E. Kenney, J. P. Basilion and C. Burda, Deep Penetration of a PDT Drug into Tumors by Noncovalent Drug-Gold Nanoparticle Conjugates, *J. Am. Chem. Soc.*, 2011, **133**, 2583–2591.

92 A. M. Master, Y. Qi, N. L. Oleinick and A. Sen Gupta, EGFR-mediated intracellular delivery of *Pc* 4 nanoformulation for targeted photodynamic therapy of cancer: in vitro studies, *Nanomedicine*, 2012, **8**, 655–664.

93 D. C. Soler, J. Ohtola, H. Sugiyama, M. E. Rodriguez, L. Han, N. L. Oleinick, M. Lam, E. D. Baron, K. D. Cooper and T. S. McCormick, Activated T cells exhibit increased uptake of silicon phthalocyanine *Pc* 4 and increased susceptibility to *Pc* 4-photodynamic therapy-mediated cell death, *Photochem. Photobiol. Sci.*, 2016, **15**, 822–831.

94 A. M. Master, M. Livingston, N. L. Oleinick and A. Sen Gupta, Optimization of a Nanomedicine-Based Silicon Phthalocyanine 4 Photodynamic Therapy (*Pc* 4-PDT) Strategy for Targeted Treatment of EGFR-Overexpressing Cancers, *Mol. Pharm.*, 2012, **9**, 2331–2338.

95 X.-M. Shen, B.-Y. Zheng, X.-R. Huang, L. Wang and J.-D. Huang, The first silicon(iv) phthalocyanine–nucleoside conjugates with high photodynamic activity, *Dalton Trans.*, 2013, **42**, 10398–10403.

96 M. K. Burdette, R. Jenkins, Y. Bandera, R. R. Powell, T. F. Bruce, X. Yang, Y. Wei and S. H. Foulger, Bovine serum albumin coated nanoparticles for in vitro activated fluorescence, *Nanoscale*, 2016, **8**, 20066–20073.

97 J.-J. Chen, Y.-Z. Huang, M.-R. Song, Z.-H. Zhang and J.-P. Xue, Silicon Phthalocyanines Axially Disubstituted with Erlotinib toward Small-Molecular-Target-Based Photodynamic Therapy, *ChemMedChem*, 2017, **12**, 1504–1511.

98 K. Li, L. Qiu, Q. Liu, G. Lv, X. Zhao, S. Wang and J. Lin, Conjugate of biotin with silicon(iv) phthalocyanine for tumor-targeting photodynamic therapy, *J. Photochem. Photobiol. B*, 2017, **174**, 243–250.

99 X.-H. Peng, S.-F. Chen, B.-Y. Zheng, B.-D. Zheng, Q.-F. Zheng, X.-S. Li, M.-R. Ke and J.-D. Huang, Comparison between amine-terminated phthalocyanines and their chlorambucil conjugates: Synthesis, spectroscopic properties, and in vitro anticancer activity, *Tetrahedron*, 2017, **73**, 378–384.

100 A. M. L. Hossion, M. Bio, G. Nkepang, S. G. Awuah and Y. You, Visible Light Controlled Release of Anticancer Drug through Double Activation of Prodrug, *ACS Med. Chem. Lett.*, 2013, **4**, 124–127.

101 M. Bio, P. Rajaputra, G. Nkepang and Y. You, Far-Red Light Activatable, Multifunctional Prodrug for Fluorescence Optical Imaging and Combinational Treatment, *J. Med. Chem.*, 2014, **57**, 3401–3409.

102 G. Nkepang, M. Bio, P. Rajaputra, S. G. Awuah and Y. You, Folate receptor-mediated enhanced and specific delivery of far-red light-activatable prodrugs of combretastatin A-4 to FR-positive tumor, *Bioconjugate Chem.*, 2014, **25**, 2175–2188.

103 P. Thapa, M. Li, M. Bio, P. Rajaputra, G. Nkepang, Y. Sun, S. Woo and Y. You, Far-Red Light-Activatable Prodrug of Paclitaxel for the Combined Effects of Photodynamic Therapy and Site-Specific Paclitaxel Chemotherapy, *J. Med. Chem.*, 2016, **59**, 3204–3214.

104 T. Doane, Y. Cheng, N. Sodhi and C. Burda, NIR Photocleavage of the Si-C Bond in Axial Si-Phthalocyanines, *J. Phys. Chem. A*, 2014, **118**, 10587–10595.

105 B. Maiti, A. K. Manna, C. McCleese, T. L. Doane, S. Chakrapani, C. Burda and B. D. Dunietz, Photoinduced Homolytic Bond Cleavage of the Central Si-C Bond in Porphyrin Macrocycles Is a Charge Polarization Driven Process, *J. Phys. Chem. A*, 2016, **120**, 7634–7640.

106 E. D. Anderson, S. Sova, J. Ivanic, L. Kelly and M. J. Schnermann, Defining the conditional basis of silicon phthalocyanine near-IR ligand exchange, *Phys. Chem. Chem. Phys.*, 2018, **20**, 19030–19036.

107 L. C. Gomes-da-Silva, O. Kepp and G. Kroemer, Regulatory approval of photoimmunotherapy: photodynamic therapy that induces immunogenic cell death, *OncolImmunology*, 2020, **9**, 1841393.

108 K. Ito, M. Mitsunaga, T. Nishimura, M. Saruta, T. Iwamoto, H. Kobayashi and H. Tajiri, Near-Infrared Photochemoimmunotherapy by Photoactivatable Bifunctional Antibody–Drug Conjugates Targeting Human Epidermal Growth Factor Receptor 2 Positive Cancer, *Bioconjugate Chem.*, 2017, **28**, 1458–1469.

109 M. Kobayashi, M. Harada, H. Takakura, K. Ando, Y. Goto, T. Tsuneda, M. Ogawa and T. Taketsugu, Theoretical and Experimental Studies on the Near-Infrared Photoreaction Mechanism of a Silicon Phthalocyanine Photoimmunotherapy Dye: Photoinduced Hydrolysis by Radical Anion Generation, *ChemPlusChem*, 2020, **85**, 1959–1963.

110 X. Li, X.-H. Peng, B.-D. Zheng, J. Tang, Y. Zhao, B.-Y. Zheng, M.-R. Ke and J.-D. Huang, New application of phthalocyanine molecules: from photodynamic therapy to photothermal therapy by means of structural regulation rather than formation of aggregates, *Chem. Sci.*, 2018, **9**, 2098–2104.

111 T. M. Grant, D. S. Josey, K. L. Sampson, T. Mudigonda, T. P. Bender and B. H. Lessard, Boron Subphthalocyanines and Silicon Phthalocyanines for Use as Active Materials in Organic Photovoltaics, *Chem. Rec.*, 2019, **19**, 1093–1112.

112 S. Honda, H. Ohkita, H. Benten and S. Ito, Multi-colored dye sensitization of polymer/fullerene bulk heterojunction solar cells, *Chem. Commun.*, 2010, **46**, 6596–6598.

113 S. Honda, H. Ohkita, H. Benten and S. Ito, Selective Dye Loading at the Heterojunction in Polymer/Fullerene Solar Cells, *Adv. Energy Mater.*, 2011, **1**, 588–598.

114 S. Honda, S. Yokoya, H. Ohkita, H. Benten and S. Ito, Light-Harvesting Mechanism in Polymer/Fullerene/Dye Ternary Blends Studied by Transient Absorption Spectroscopy, *J. Phys. Chem. C*, 2011, **115**, 11306–11317.



115 L. Ke, J. Min, M. Adam, N. Gasparini, Y. Hou, J. D. Perea, W. Chen, H. Zhang, S. Fladischer, A.-C. Sale, E. Spiecker, R. R. Tykwinski, C. J. Brabec and T. Ameri, A Series of Pyrene-Substituted Silicon Phthalocyanines as Near-IR Sensitizers in Organic Ternary Solar Cells, *Adv. Energy Mater.*, 2016, **6**, 1502355.

116 B. Lim, J. T. Bloking, A. Ponec, M. D. McGehee and A. Sellinger, Ternary Bulk Heterojunction Solar Cells: Addition of Soluble NIR Dyes for Photocurrent Generation beyond 800 nm, *ACS Appl. Mater. Interfaces*, 2014, **6**, 6905–6913.

117 L. Ke, N. Gasparini, J. Min, H. Zhang, M. Adam, S. Rechberger, K. Forberich, C. Zhang, E. Spiecker, R. R. Tykwinski, C. J. Brabec and T. Ameri, Panchromatic ternary/quaternary polymer/fullerene BHJ solar cells based on novel silicon naphthalocyanine and silicon phthalocyanine dye sensitizers, *J. Mater. Chem. A*, 2017, **5**, 2550–2562.

118 B. Lim, G. Y. Margulis, J.-H. Yum, E. L. Unger, B. E. Hardin, M. Grätzel, M. D. McGehee and A. Sellinger, Silicon-Naphthalo/Phthalocyanine-Hybrid Sensitizer for Efficient Red Response in Dye-Sensitized Solar Cells, *Org. Lett.*, 2013, **15**, 784–787.

119 B. H. Lessard, T. M. Grant, R. White, E. Thibau, Z.-H. Lu and T. P. Bender, The position and frequency of fluorine atoms changes the electron donor/acceptor properties of fluorophenoxy silicon phthalocyanines within organic photovoltaic devices, *J. Mater. Chem. A*, 2015, **3**, 24512–24524.

120 E. Zysman-Colman, S. S. Ghosh, G. Xie, S. Varghese, M. Chowdhury, N. Sharma, D. B. Cordes, A. M. Z. Slawin and I. D. W. Samuel, Solution-Processable Silicon Phthalocyanines in Electroluminescent and Photovoltaic Devices, *ACS Appl. Mater. Interfaces*, 2016, **8**, 9247–9253.

121 T. M. Grant, T. Gorisse, O. Dautel, G. Wantz and B. H. Lessard, Multifunctional ternary additive in bulk heterojunction OPV: increased device performance and stability, *J. Mater. Chem. A*, 2017, **5**, 1581–1587.

122 A. J. Pearson, T. Plint, S. T. E. Jones, B. H. Lessard, D. Credgington, T. P. Bender and N. C. Greenham, Silicon phthalocyanines as dopant red emitters for efficient solution processed OLEDs, *J. Mater. Chem. C*, 2017, **5**, 12688–12698.

123 P. Gawrys, T. Marszalek, E. Bartnik, M. Kucinska, J. Ulanski and M. Zagorska, Novel, Low-Cost, Highly Soluble n-Type Semiconductors: Tetraazaanthracene Tetraesters, *Org. Lett.*, 2011, **13**, 6090–6093.

124 N. T. Boileau, O. A. Melville, B. Mirka, R. Cranston and B. H. Lessard, P and N type copper phthalocyanines as effective semiconductors in organic thin-film transistor based DNA biosensors at elevated temperatures, *RSC Adv.*, 2019, **9**, 2133–2142.

125 O. A. Melville, T. M. Grant and B. H. Lessard, Silicon phthalocyanines as N-type semiconductors in organic thin film transistors, *J. Mater. Chem. C*, 2018, **6**, 5482–5488.

126 O. A. Melville, T. M. Grant, K. Lochhead, B. King, R. Ambrose, N. A. Rice, N. T. Boileau, A. J. Peltekoff, M. Tousignant, I. G. Hill and B. H. Lessard, Contact Engineering Using Manganese, Chromium, and Bathocuproine in Group 14 Phthalocyanine Organic Thin-Film Transistors, *ACS Appl. Electron. Mater.*, 2020, **2**, 1313–1322.

127 O. A. Melville, T. M. Grant, B. Mirka, N. T. Boileau, J. Park and B. H. Lessard, Ambipolarity and Air Stability of Silicon Phthalocyanine Organic Thin-Film Transistors, *Adv. Electron. Mater.*, 2019, **5**, 1900087.

128 G. Knör and U. Monkowius, Photosensitization and photocatalysis in bioinorganic, bio-organometallic and biomimetic systems, *Adv. Inorg. Chem.*, 2011, **63**, 235–289.

129 R. Menting, J. T. F. Lau, H. Xu, D. K. P. Ng, B. Röder and E. A. Ermilov, Formation and photoinduced processes of a self-assembled subphthalocyanine–porphyrin–phthalocyanine supramolecular complex, *Chem. Commun.*, 2012, **48**, 4597–4599.

130 S. Zhu and D. Wang, Photocatalysis: Basic Principles, Diverse Forms of Implementations and Emerging Scientific Opportunities, *Adv. Energy Mater.*, 2017, **7**, 1700841.

131 C. Uslan, K. T. Oppelt, L. M. Reith, B. S. Sesalan and G. Knör, Characterization of a non-aggregating silicon(IV) phthalocyanine in aqueous solution: toward red-light-driven photocatalysis based on earth-abundant materials, *Chem. Commun.*, 2013, **49**, 8108–8110.

132 E. T. Saka, H. Yalazan, Z. Biyiklioglu, H. Kantekin and K. Tekintas, Synthesis, aggregation, photocatalytical and electrochemical properties of axially 1-benzylpiperidin-4-oxy units substituted silicon phthalocyanine, *J. Mol. Struct.*, 2020, **1199**, 126994.

133 J. Huang, Y. Wu, D. Wang, Y. Ma, Z. Yue, Y. Lu, M. Zhang, Z. Zhang and P. Yang, Silicon Phthalocyanine Covalently Functionalized N-Doped Ultrasmall Reduced Graphene Oxide Decorated with Pt Nanoparticles for Hydrogen Evolution from Water, *ACS Appl. Mater. Interfaces*, 2015, **7**, 3732–3741.

134 B. Xiao, M. Zhu, X. Li, P. Yang, L. Qiu and C. Lu, A stable and efficient photocatalytic hydrogen evolution system based on covalently linked silicon-phthalocyanine-graphene with surfactant, *Int. J. Hydrogen Energy*, 2016, **41**, 11537–11546.

